SOURCE ESTIMATION WITH INCOHERENT WAVES IN RANDOM WAVEGUIDES

SEBASTIAN ACOSTA*, RICARDO ALONSO† AND LILIANA BORCEA‡

Abstract. We study an inverse source problem for the acoustic wave equation in a random waveguide. The goal is to estimate the source of waves from measurements of the acoustic pressure at a remote array of sensors. The waveguide effect is due to boundaries that trap the waves and guide them in a preferred (range) direction, the waveguide axis, along which the medium is unbounded. The random waveguide is a model of perturbed ideal waveguides which have flat boundaries and are filled with known media that do not change with range. The perturbation consists of fluctuations of the boundary and of the wave speed due to numerous small inhomogeneities in the medium. The fluctuations are uncertain in applications, which is why we model them with random processes, and they cause significant cumulative scattering at long ranges from the source. The scattering effect manifests mathematically as an exponential decay of the expectation of the acoustic pressure, the coherent part of the wave. The incoherent wave is modeled by the random fluctuations of the acoustic pressure, which dominate the expectation at long ranges from the source. We use the existing theory of wave propagation in random waveguides to analyze the inverse problem of estimating the source from incoherent wave recordings at remote arrays. We show how to obtain from the incoherent measurements high fidelity estimates of the time resolved energy carried by the waveguide modes, and study the invertibility of the system of transport equations that model energy propagation in order to estimate the source.

Key words. Waveguides, random media, transport equations, Wigner transform.

AMS subject classifications. 35Q61, 35R60

1. Introduction.

We study an inverse problem for the scalar (acoustic) wave equation, where we wish to estimate the source of waves from measurements of the acoustic pressure field $p(t, \vec{\mathbf{x}})$ at a remote array of receiver sensors. The waves propagate in a waveguide, meaning that they are trapped by boundaries and are guided in the range direction, the waveguide axis, along which the medium is unbounded. Ideally the boundaries are straight and the medium does not change with range. We consider perturbed waveguides filled with heterogeneous media, where the boundary and the wave speed have small fluctuations on scales similar to the wavelength. These fluctuations have little effect in the vicinity of the source, but they are important at long ranges because they cause significant cumulative wave scattering. We suppose that the array of receivers is far from the source, as is typical in applications in underwater acoustics, sound propagation in corrugated pipes, in tunnels, etc., and study how cumulative scattering impedes the inversion.

In most setups the fluctuations are uncertain, which is why we introduce a stochastic framework and model them with random processes. The inversion is carried in only one perturbed waveguide, meaning that the array measures one realization of the random pressure field, the solution of the wave equation in that waveguide. The stochastic framework allows us to study the chain of mappings from the uncertainty in the waveguide to the uncertainty of the array measurements and of the inversion results. The goal is to understand how to process the uncertain data and quantify what can be estimated about the source in a reliable (statistically stable) manner. Statistical stability means that the estimates do not change with the realization of the fluctuations of the waveguide, which are unknown.

*Baylor College of Medicine, Houston, TX 77005. sacosta@bcm.edu

†Departamento de Matemática, PUC–Rio, Brasil. ralonso@mat.puc-rio.br

‡Department of Mathematics, University of Michigan, Ann Arbor, MI 48109. borcea@umich.edu

The problem of imaging (localizing) sources in waveguides has been studied extensively in underwater acoustics [5, 19, 17, 1]. Typical imaging approaches are matched field and related coherent methods that match the measured $p(t, \vec{\mathbf{x}})$ with its mathematical model for search locations of the source. The model is based on wave propagation in ideal waveguides and the imaging is successful when $p(t, \vec{\mathbf{x}})$ is mostly coherent. The coherent part of $p(t, \vec{\mathbf{x}})$ is its statistical expectation $\mathbb{E}[p(t, \vec{\mathbf{x}})]$ with respect to realizations of the random waveguide, and the incoherent field is modeled by $p(t, \vec{\mathbf{x}}) - \mathbb{E}[p(t, \vec{\mathbf{x}})]$. As the waves propagate in the random waveguide they lose coherence due to scattering by the fluctuations of the boundary and the inhomogeneities in the medium. This manifests as an exponential decay in range of the expectation $\mathbb{E}[p(t, \vec{\mathbf{x}})]$, and strengthening of the fluctuations $p(t, \vec{\mathbf{x}}) - \mathbb{E}[p(t, \vec{\mathbf{x}})]$.

Detailed studies of the loss of coherence of sound waves due to cumulative scattering are given in [18, 10, 12, 16, 13] for waveguides filled with randomly heterogeneous media and in [4, 15] for waveguides with random boundaries. These waveguides are two dimensional models of the ocean, and they may leak (radiate) in the ocean floor. The problem is similar in three dimensional acoustic waveguides with bounded cross-section. We refer to [7] for wave propagation in three dimensional waveguide models of the ocean which have unbounded cross-section and random pressure release top boundary, and to [3, 20] for three dimensional electromagnetic random waveguides. In all cases the analysis of loss of coherence is based on the decomposition of the wave field in an infinite set of monochromatic waves called waveguide modes, which are special solutions of the wave equation in the ideal waveguide. Finitely many modes are propagating waves, and we may associate them with plane waves that strike the boundary at different angles of incidence and are reflected repeatedly. The remaining infinitely many modes are evanescent and/or radiating waves. The cumulative scattering in the waveguide is modeled by the amplitude of the modes. When the scattering is weak, as is the case at moderate distances from the source, the amplitudes are approximately constant in range, and they are determined solely by the source excitation. Scattering builds up over long ranges and the mode amplitudes become random fields with exponentially decaying expectation on range scales called scattering mean free paths.

The mode dependence of the scattering mean free paths is analyzed in [4]. It turns out that the slow modes, which correspond to plane waves that strike the boundary at almost normal incidence, are most affected by scattering. These waves have long trajectories from the source to the array, and thus interact more with the boundary and medium fluctuations. The scattering mean free paths have a more pronounced mode dependence when the boundary fluctuations dominate those of the medium. They are much longer for the fast modes which correspond to plane waves that hit the boundary at small (grazing) angles and have fewer interactions with the boundary fluctuations on their almost direct trajectories from the source to the array. Therefore, it is possible to improve coherent imaging methods in waveguides with random boundaries by filtering out the incoherent slow mode components of the array data. This is shown in [8] with numerical simulations and analysis based on the theory in [18, 12, 4]. See also the results in [19, 17, 23].

When the array is further from the source than the scattering mean free paths of all the modes, the data is incoherent and coherent imaging methods like matched field cannot work. In this paper we assume that this is the case and study an inversion approach based on a system of transport equations that models the propagation of energy carried by the modes. This system is derived in [18, 12, 4] and is used in

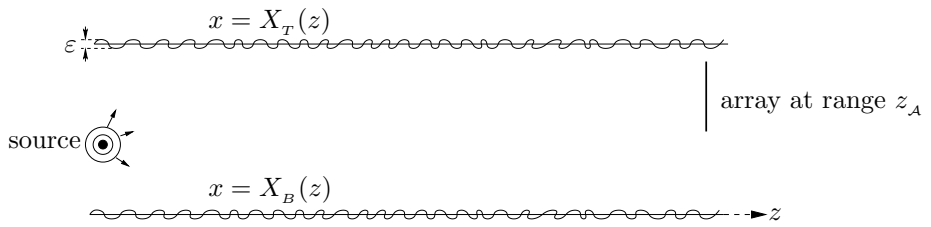

FIG. 2.1. *Schematic of the problem setup. The source emits a signal in a waveguide and the wave field is recorded at a remote array. The perturbed waveguide has fluctuating boundaries and is filled with a medium with fluctuating wave speed.*

[9] to estimate the location of a point source in random waveguides. Here we study the inverse problem in more detail and answer the following questions: (1) How can we obtain reliable estimates of the mode energies from the incoherent pressure field measured at the array? (2) What kind of information about the source can we recover from the transport equations? (3) Can we quantify the deterioration of the inversion results in terms of the range offset between the source and the array?

We begin in section 2 with the mathematical formulation of the inverse problem, and recall in section 3 the model of the random wave field $p(t, \vec{\mathbf{x}})$ derived in [18, 12, 4, 6]. The main results of the paper are in section 4. We motivate there the inversion based on energy transport, and describe the forward mapping from the source to the expectation of the time resolved energy carried by the modes. We show how to calculate this energy from the incoherent array data, and describe how to invert approximately the transport equations. The results quantify the limited information about the source that can be recovered with a given array. We end with a summary and discussion in section 5.

2. Formulation of the problem. We limit our study to two dimensional waveguides with reflecting boundaries modeled by pressure release boundary conditions. This is for simplicity, but the results should extend to other boundary conditions and to leaky and three dimensional waveguides, as discussed in section 5. We illustrate the setup in Figure 2.1, and introduce the system of coordinates $\vec{\mathbf{x}} = (x, z)$ with range z originating from the center of the source. The waveguide occupies the domain

$$\Omega = \{\vec{\mathbf{x}} = (x, z) : \quad x \in (X_{_B}(z), X_{_T}(z)), \quad z \in \mathbb{R}\},$$

where the cross-range x takes values between the bottom and top boundaries modeled by $X_{_B}(z)$ and $X_{_T}(z)$. The source has an unknown density $\rho(\vec{\mathbf{x}})$ which is compactly supported in Ω, near $z = 0$, and emits a signal $F(t)$ which is a pulse $f(Bt)$ of support of order $1/B$ around $t = 0$, modulated by an oscillatory exponential

$$F(t) = e^{-i\omega_o t} f(Bt). \tag{2.1}$$

We introduce the bandwidth B in the argument of the pulse to emphasize that the Fourier transform $\widehat{F}(\omega)$ of the signal is supported in an interval of order B around the central frequency ω_o,

$$\widehat{F}(\omega) = \int_{-\infty}^{\infty} dt\, F(t) e^{i\omega t} = \frac{1}{B} \widehat{f}\left(\frac{\omega - \omega_o}{B}\right). \tag{2.2}$$

The array is a collection of receivers that are placed close together in the set

$$A = \{\vec{\mathbf{x}}_{_{\mathcal{A}}} = (x, z_{_{\mathcal{A}}}) : \quad x \in \mathcal{A} \subset [X_{_B}(z), X_{_T}(z)]\},$$

at range $z_{\mathcal{A}} > 0$ from the source, where $\mathcal{A}$ is an interval called the array aperture. The receivers record the acoustic pressure field $p(t, \vec{\mathbf{x}})$ modeled by the solution of the acoustic wave equation

$$\left[\partial_x^2 + \partial_z^2 - c^{-2}(\vec{\mathbf{x}})\partial_t^2\right] p(t, \vec{\mathbf{x}}) = F(t)\rho(\vec{\mathbf{x}}), \quad \vec{\mathbf{x}} \in \Omega, \quad t > 0, \tag{2.3}$$

with pressure release boundary conditions

$$p(t, \vec{\mathbf{x}}) = 0, \quad t > 0, \quad \vec{\mathbf{x}} \in \partial\Omega = \{\vec{\mathbf{x}} = (x, z) : \quad x \in \{X_{\scriptscriptstyle B}(z), X_{\scriptscriptstyle T}(z)\}, \quad z \in \mathbb{R}\}, \tag{2.4}$$

and initial condition $p(t, \vec{\mathbf{x}}) \equiv 0$ for $t \ll 0$. Here $c(\vec{\mathbf{x}})$ is the sound speed.

The inverse problem is to determine the source density $\rho(\vec{\mathbf{x}})$ from the array data recordings $D(t, x)$. We model them by

$$D(t, x) = p(t, \vec{\mathbf{x}}_{\mathcal{A}}) 1_{\mathcal{A}}(x) \chi\left(\frac{t - t_o}{\mathcal{T}}\right), \quad \vec{\mathbf{x}}_{\mathcal{A}} = (x, z_{\mathcal{A}}), \tag{2.5}$$

using a recording time window χ centered at t_o and of duration $\mathcal{T}$. We also approximate the array by a continuum aperture in the interval $\mathcal{A}$, and use the indicator function $1_{\mathcal{A}}(x)$ which equals one when $x \in \mathcal{A}$ and zero otherwise.

2.1. The random model of perturbed waveguides. In ideal waveguides the sound speed is modeled by a function $c_o(x)$ that is independent of range and the boundaries are straight, meaning that $X_{\scriptscriptstyle B}(z) = 0$ and $X_{\scriptscriptstyle T}(z) = X$, a constant. The sound speed in the perturbed waveguide fluctuates around c_o and the boundaries $X_{\scriptscriptstyle B}$ and $X_{\scriptscriptstyle T}$ fluctuate around 0 and X. The fluctuations are assumed on scales that are comparable to the central wavelength λ_o, so they interact efficiently with the waves and give significant long range net scattering even though they have small amplitude. We quantify this amplitude with a positive dimensionless parameter $\varepsilon \ll 1$, which is used in [18, 12, 4, 6] to analyze the pressure field at properly scaled ranges, in the asymptotic limit $\varepsilon \to 0$.

We take c_o constant for simplicity, to write explicitly the mode decomposition, but the results extend easily to cross-range dependent $c_o(x)$. The perturbed sound speed $c(\vec{\mathbf{x}})$ is modeled by

$$\frac{1}{c^2(\vec{\mathbf{x}})} = \frac{1}{c_o^2}\left[1 + \varepsilon\nu\left(\frac{\vec{\mathbf{x}}}{\ell}\right)\right], \tag{2.6}$$

where ν is a mean zero random process that is bounded almost surely, so that the right hand side in (2.6) remains positive. We assume that ν is stationary and mixing in range, meaning in particular that the auto-correlation

$$\mathcal{R}_\nu(\xi, \xi', \eta) = \mathbb{E}\left[\nu(\xi, u)\nu(\xi', u + \eta)\right] \tag{2.7}$$

is absolutely integrable in the third argument over the real line. The process ν is normalized by $\mathcal{R}_\nu(0, 0, 0) = 1$ and

$$\int_{-\infty}^{\infty} dz\, \mathcal{R}_\nu\left(\frac{x}{\ell}, \frac{x'}{\ell}, \frac{z}{\ell}\right) = O(\ell),$$

where ℓ is the correlation length, the range offset over which the random fluctuations become statistically decorrelated. The scaling by the same ℓ of the cross-range in (2.6)

means that the heterogeneous medium is isotropic, but we could have $\ell_X = O(\ell)$ as well, without changing the conclusions.

We model similarly the boundary fluctuations

$$X_{_B}(z) = \varepsilon\mu_{_B}\left(\frac{z}{\ell}\right), \qquad X_{_T}(z) = X\left[1+\varepsilon\mu_{_T}\left(\frac{z}{\ell}\right)\right], \tag{2.8}$$

using two mean zero, stationary and mixing random processes $\mu_{_B}$ and $\mu_{_T}$, that are bounded almost surely and have integrable autocorrelation $\mathcal{R}_{_B}$ and $\mathcal{R}_{_T}$. We use the same correlation length ℓ to simplify notation, but the results hold for any scales $\ell_{_B}$ and $\ell_{_T}$ of the order of ℓ. For technical reasons related to the method of analysis used in [4] we also assume that the processes $\mu_{_B}$ and $\mu_{_T}$ have bounded first and second derivatives, almost surely. Less smooth boundary fluctuations are considered in [15].

The theory of wave propagation in waveguides with long range correlations of the random fluctuations of $c(\vec{\mathbf{x}})$ is being developed [14], and our results are expected to extend (with modifications) to such settings. The case of turning waveguides with smooth and large variations of the boundaries, on scales that are comparable to $z_{_{\mathcal{A}}}$, is much more difficult. The analysis of wave propagation in such waveguides is quite involved [22, 11, 2] and the mapping of random fluctuations of the sound speed to $p(t,\vec{\mathbf{x}})$ is not understood in detail, although it is considered formally in [20].

3. Cumulative scattering effects in the random waveguide. We write the solution of the wave equation (2.3)-(2.4) as

$$p(t,\vec{\mathbf{x}}) = \int_{\Omega_\rho} d\vec{\mathbf{x}}'\,\rho(\vec{\mathbf{x}}')p(t,\vec{\mathbf{x}},\vec{\mathbf{x}}'), \tag{3.1}$$

where $p(t,\vec{\mathbf{x}},\vec{\mathbf{x}}')$ is the wave field due to a point source at $\vec{\mathbf{x}}' = (\mathbf{x}',z')$, emitting the signal $F(t)$ defined in (2.1), and $\Omega_\rho \subset \Omega$ is the compact support of the source, which lies near $z'=0$. The points $\vec{\mathbf{x}} = (\mathbf{x},z)$ in (3.1) are at range $z > z'$, for all $\vec{\mathbf{x}}' \in \Omega_\rho$.

It follows from [18, 12, 4, 6] that $p(t,\vec{\mathbf{x}},\vec{\mathbf{x}}')$ is a linear superposition of propagating and evanescent waves, called waveguide modes

$$p(t,\vec{\mathbf{x}},\vec{\mathbf{x}}') = \int_{-\infty}^{\infty}\frac{d\omega}{2\pi B}\widehat{f}\left(\frac{\omega-\omega_o}{B}\right)e^{-i\omega t}\Big[\sum_{j=1}^{N}a_j^+(\omega,z,\vec{\mathbf{x}}')\Psi_j^+(\omega,x,z-z')+$$
$$\sum_{j=1}^{N}a_j^-(\omega,z,\vec{\mathbf{x}}')\Psi_j^-(\omega,x,z-z') + \sum_{j=N+1}^{\infty}a_j^e(\omega,z,\vec{\mathbf{x}}')\Psi_j^e(\omega,x,z-z')\Big]. \tag{3.2}$$

The modes are special solutions of the wave equation in the ideal waveguide, and can be obtained with separation of variables. There are $2N$ propagating modes

$$\Psi_j^{\pm}(\omega,x,z-z') = \phi_j(x)e^{\pm i\beta_j(\omega)(z-z')}, \quad j=1,\ldots.N, \tag{3.3}$$

with index + denoting forward going and − backward going, and infinitely many evanescent modes

$$\Psi_j^e(\omega,x,z-z') = \phi_j(x)e^{-\beta_j(\omega)|z-z'|}, \quad j>N. \tag{3.4}$$

They are defined by the complete and orthonormal set $\{\phi_j(x)\}_{j\geq 1}$ of eigenfunctions of the symmetric linear operator $\mathbb{L}_x = \partial_x^2 + \omega^2/c_o^2$ with homogeneous Dirichlet boundary conditions at $x=0$ and $x=X$. Because c_o is constant we can write

$$\phi_j(x) = \sqrt{\frac{2}{X}}\sin\left(\frac{\pi j x}{X}\right), \tag{3.5}$$

and note explicitly how Ψ_j^+ are associated with monochromatic plane waves that travel in the direction of the slowness vectors $(\pm\pi j/X, \beta_j)$ and strike the boundaries where they reflect according to Snell's law. The mode wavenumbers are denoted by $\beta_j(\omega)$, and are determined by the square root of the eigenvalues of the operator $\mathbb{L}_x$

$$\beta_j(\omega) = \left| k^2 - \left(\frac{\pi j}{X}\right)^2 \right|^{1/2}, \tag{3.6}$$

where $k = \omega/c_o$. The β_j of the propagating modes correspond to the first N eigenvalues which are positive, where

$$N(\omega) = \left\lfloor \frac{kX}{\pi} \right\rfloor \tag{3.7}$$

and $\lfloor\cdot\rfloor$ denotes the integer part.

We assume for simplicity that the bandwidth B is not too large, which is typical in applications in underwater acoustics, so that there is the same number of propagating modes for all the frequencies of the pulse, and drop the dependence of N on ω. We also suppose that there are no standing waves, meaning that β_j are bounded below by a positive constant, for all $j \geq 1$.

The cumulative scattering effects in the random waveguide are modeled by the mode amplitudes $\{a_j^{\pm}(\omega, z, \vec{\mathbf{x}}')\}_{1\leq j\leq N}$ and $\{a_j^e(\omega, z, \vec{\mathbf{x}}')\}_{j>N}$, which are random fields. In ideal waveguides the amplitudes are constant in range for $z > z'$

$$a_{j,o}^+(\omega, \vec{\mathbf{x}}') = \frac{\phi_j(x')}{2i\beta_j(\omega)}, \qquad j = 1, \ldots, N, \tag{3.8}$$

$$a_{j,o}^-(\omega, \vec{\mathbf{x}}') = 0, \qquad j = 1, \ldots, N, \tag{3.9}$$

$$a_{j,o}^e(\omega, \vec{\mathbf{x}}') = -\frac{\phi_j(x')}{2\beta_j(\omega)}, \qquad j > N. \tag{3.10}$$

They depend on the cross-range x' in the support of the source, and (3.9) complies with the wave being outgoing. In random waveguides the mode amplitudes satisfy a coupled system of stochastic differential equations driven by the random fluctuations ν, $\mu_{_B}$ and $\mu_{_T}$. They are analyzed in detail in [18, 12, 4, 6] and the result is that they are approximately the same as (3.8)-(3.10) for range offsets $z - z' \ll \lambda_o/\varepsilon^2$. This motivates the long range scaling

$$z_{_\mathcal{A}} = \frac{Z_{_\mathcal{A}}}{\varepsilon^2}, \tag{3.11}$$

where cumulative scattering becomes significant. The evanescent modes may be neglected at such ranges[1], and we use a further approximation that neglects the backward going waves to write

$$p(t, \vec{\mathbf{x}}, \vec{\mathbf{x}}') \approx \int_{-\infty}^{\infty} \frac{d\omega}{2\pi B} \widehat{f}\left(\frac{\omega - \omega_o}{B}\right) e^{-i\omega t} \sum_{j=1}^{N} a_j^+(\omega, z, \vec{\mathbf{x}}')\phi_j(x) e^{i\beta_j(\omega)(z-z')}. \tag{3.12}$$

[1]Note that although the evanescent modes do not appear explicitly in (3.12), they affect the amplitudes of the propagating modes. This amplitude coupling is taken into account in the analysis in [18, 12, 4, 6] and thus in the results of this paper.

The forward scattering approximation is justified by the fact that the backward mode amplitudes have very weak coupling with the forward ones, for autocorrelations of the fluctuations that are smooth enough in z [18, 12, 4, 6]. We refer to [13] for the analysis of wave propagation that includes both the forward and backward going modes, but for the purpose of this paper it suffices to use (3.12).

Let us write the amplitudes a_j^+ using the random propagator $\mathbb{P}^\varepsilon \in \mathbb{C}^{N\times N}$, which maps the amplitudes (3.8) near the source at range z', to those at the array

$$a_j^+\left(\omega, \frac{Z_{\mathcal{A}}}{\varepsilon^2}, \vec{\mathbf{x}}'\right) = \sum_{l=1}^N \mathbb{P}^\varepsilon_{jl}(\omega, Z_{\mathcal{A}}, z')\frac{\phi_l(x')}{2i\beta_l(\omega)}. \tag{3.13}$$

The propagator is analyzed in [18, 12, 4] in the asymptotic limit $\varepsilon \to 0$. It converges in distribution to a Markov diffusion $\mathbb{P}$ with generator computed explicitly in terms of the autocorrelations of the random fluctuations. Thus, we can rewrite (3.13) as

$$a_j^+\left(\omega, \frac{Z_{\mathcal{A}}}{\varepsilon^2}, \vec{\mathbf{x}}'\right) \sim \sum_{l=1}^N \mathbb{P}_{jl}(\omega, Z_{\mathcal{A}}, z')\frac{\phi_l(x')}{2i\beta_l(\omega)}, \tag{3.14}$$

with symbol $\sim$ denoting approximate in distribution. It means that we can approximate the statistical moments of a_j^+ using the right hand side in (3.14), with an $o(1)$ error in the limit $\varepsilon \to 0$.

3.1. Data model. The data model follows from (2.5), (3.1) and (3.12)

$$D(t,x) \approx \int_{\Omega_\rho} d\vec{\mathbf{x}}'\rho(\vec{\mathbf{x}}')\int_{-\infty}^{\infty}\frac{du}{2\pi}\,\widehat{\chi}(u)\,e^{iu\frac{t_o}{\mathcal{T}}}\int_{-\infty}^{\infty}\frac{d\omega}{2\pi B}\widehat{f}\left(\frac{\omega-\omega_o}{B}-\frac{u}{B\mathcal{T}}\right)e^{-i\omega t}\times$$
$$\sum_{j=1}^N 1_{\mathcal{A}}(x)\phi_j(x)\,a_j^+\left(\omega-\frac{u}{\mathcal{T}}, \frac{Z_{\mathcal{A}}}{\varepsilon^2}, \vec{\mathbf{x}}'\right)e^{i\beta_j\left(\omega-\frac{u}{\mathcal{T}}\right)\left(\frac{Z_{\mathcal{A}}}{\varepsilon^2}-z'\right)}, \tag{3.15}$$

where $\widehat{\chi}$ is the Fourier transform of the recording window and a_j^+ is given by (3.13)-(3.14). We take henceforth the bandwidth

$$B = \omega_o\varepsilon^\alpha, \quad 1<\alpha<2, \tag{3.16}$$

which is small with respect to the center frequency. We ask that $\alpha < 2$ because the travel time of the modes is of order ε^{-2}, and we need a pulse of much smaller temporal support in order to distinguish the arrival time of different modes. That $\alpha < 2$ is also needed for the statistical stability of the inversion, as we explain later. The choice $\alpha > 1$ is for convenience, because it allows us to linearize the phase in (3.15) as

$$\beta_j\left(\omega-\frac{u}{\mathcal{T}}\right)\left(\frac{Z_{\mathcal{A}}}{\varepsilon^2}-z'\right) \approx \left[\beta_j\left(\omega_o\right)+\left(\omega-\omega_o-\frac{u}{\mathcal{T}}\right)\beta_j'(\omega_o)\right]\left(\frac{Z_{\mathcal{A}}}{\varepsilon^2}-z'\right), \tag{3.17}$$

with small error of order $\varepsilon^{2(\alpha-1)}$. When we use this approximation in (3.15) we see that the modes propagate with range speed

$$1/\beta_j'(\omega_o) = c_o\beta_j(\omega_o)/k. \tag{3.18}$$

The mode wavenumbers β_j decrease monotonically with j, so the first modes are faster as expected, because they take a more direct path from the source to the array. For

example, in the case $N = \lfloor kX/\pi \rfloor \gg 1$ the slowness vectors $(\pm\pi/X, \beta_1)$ of the plane waves associated with the first mode are almost parallel to the range direction, and the range speed is $1/\beta_1' \approx c_o$. For the last modes the slowness vectors $(\pm\pi N/X, \beta_N)$ are almost orthogonal to the range direction and the speed is much smaller than c_o.

It is natural to choose the duration $\mathcal{T}$ of the recording window to be much longer than that of the pulse $\mathcal{T} \gg 1/B$. We shall see that in fact we need $\mathcal{T}$ to be at least of the order of the travel time of the waves in order for the incoherent imaging method to work. Thus, we let

$$\mathcal{T} = \varepsilon^{-2} T, \tag{3.19}$$

with $T \geq O(1/\omega_o)$. We also assume that $\widehat{f}$ is a continuous function to simplify (3.15) slightly using the approximation

$$\widehat{f}\left(\frac{\omega-\omega_o}{B} - \frac{u}{B\mathcal{T}}\right) = \widehat{f}\left(\frac{\omega-\omega_o}{B} - \varepsilon^{2-\alpha}\frac{u}{\omega_o T}\right) \approx \widehat{f}\left(\frac{\omega-\omega_o}{B}\right). \tag{3.20}$$

3.2. Loss of coherence. To compute the coherent part of the data model, we recall from [18, 12, 4, 6] the expectation of the limit propagator

$$\mathbb{E}\left[\mathbb{P}_{jl}(\omega, Z_{\mathcal{A}}, z')\right] \approx \delta_{jl} \exp\left[-\frac{Z_{\mathcal{A}}}{\mathcal{S}_j} + i\frac{Z_{\mathcal{A}}}{\mathcal{L}_j}\right], \tag{3.21}$$

where δ_{jl} is the Kronecker delta symbol and the approximation is due to the fact that z' is much smaller than $O(\varepsilon^{-2})$. Although the mean propagator is a diagonal matrix as in ideal waveguides, where it is the identity, its entries are exponentially damped in $Z_{\mathcal{A}}$ on scales $\mathcal{S}_j$, the scattering mean free path of the modes. There is also an anomalous phase accumulated on the mode dependent scales $\mathcal{L}_j$.

We refer to [4, 8] for details on the scales $\mathcal{S}_j$ and $\mathcal{L}_j$. It is not important to write down their expressions which can be found in [8, equations (3.19),(3.28),(3.31)] except to note that they are defined in terms of the autocorrelations $\mathcal{R}_\nu$, $\mathcal{R}_{_B}$ and $\mathcal{R}_{_T}$ of the fluctuations. Both $\mathcal{S}_j$ and $\mathcal{L}_j$ decrease monotonically with the mode index j. They are much longer for the first modes when scattering by the random boundaries dominate, and change slowly with j when the scattering is due to the medium filling the waveguide.

We assume henceforth that $Z_{\mathcal{A}} \gtrsim 3\mathcal{S}_1$, and conclude from (3.14) and (3.21) that

$$\left|\mathbb{E}\left[a_j^+\left(\omega, \frac{Z_{\mathcal{A}}}{\varepsilon^2}, \vec{\mathbf{x}}'\right)\right]\right| \leq e^{-\frac{Z_{\mathcal{A}}}{\mathcal{S}_1}} \left|a_{j,o}^+(\omega, \vec{\mathbf{x}}')\right| \ll \left|a_{j,o}^+(\omega, \vec{\mathbf{x}}')\right|, \tag{3.22}$$

for all $j = 1, \ldots, N$. Recall that $a_{j,o}^+$ is the amplitude of the modes in ideal waveguides given by (3.8). It is also the initial condition of $a_j^+(\omega, z, \vec{\mathbf{x}}')$ for $z = z'$. Equation (3.22) states that the expectation of the mode amplitudes decays exponentially with range and it is negligible in our regime. This decay is not caused by attenuation in the medium, because the wave equation conserves energy. For any frequency ω, the energy conservation relation takes the form

$$\sum_{j=1}^{N}\left|a_j^+\left(\omega, \frac{Z_{\mathcal{A}}}{\varepsilon^2}, \vec{\mathbf{x}}'\right)\right|^2 \approx \sum_{j=1}^{N}\left|a_{j,o}^+(\omega, \vec{\mathbf{x}}')\right|^2, \tag{3.23}$$

where the approximation is with an $o(1)$ error as $\varepsilon \to 0$, due to the neglect of the backward going and evanescent waves. Equation (3.23) indicates that the expectation

of the energy $|a_j^+|^2$ of the modes does not decay, a fact stated explicitly in section 4. Thus, (3.22) is a manifestation of the loss of coherence of the amplitudes, meaning that their random fluctuations dominate their expectation. The data recorded by arrays at ranges $z_{\mathcal{A}} = Z_{\mathcal{A}}/\varepsilon^2$ with $Z_{\mathcal{A}} \gtrsim 3\mathcal{S}_1$ is incoherent.

3.3. Statistical decorrelation. We just stated that some second moments of the mode amplitudes remain large. To decide if we can estimate them reliably from the incoherent data and thus use them in inversion, we need to know how the waves decorrelate. Statistical decorrelation means that the second moments of the amplitudes are equal approximately to the product of their expectations, which is very small because $Z_{\mathcal{A}} \gtrsim 3\mathcal{S}_1$.

The two frequency analysis of the propagator $\mathbb{P}^\varepsilon$ is carried out in [12, 4], and the result is that the waves are decorrelated for frequency offsets

$$|\omega - \omega'| \geq O(\varepsilon^2 \omega_o).$$

Such small offsets are enough to cause the waves to interact differently with the random fluctuations over range intervals of the order $Z_{\mathcal{A}}/\varepsilon^2$, thus giving the statistical decorrelation. This result is important because it says that we can estimate those second moments of the amplitudes that do not decay in range by cross-correlating the Fourier transform of the data at nearby frequencies, and then integrating over the bandwidth to obtain a statistically stable result. The bandwidth B is much larger than $\varepsilon^2\omega_o$ by assumption (3.16), and the statistical stability follows essentially from a law of large numbers, because we sum a large number of terms that are uncorrelated.

The second moments of the propagator at nearby frequencies are

$$\begin{aligned}\mathbb{E}\left[\mathbb{P}^\varepsilon_{jl}(\omega, Z_{\mathcal{A}}, z)\overline{\mathbb{P}^\varepsilon_{j'l'}(\omega - \varepsilon^2 h, Z_{\mathcal{A}}, z')}\right] \approx \delta_{jl}\delta_{j'l'}\frac{\beta_l(\omega)}{\beta_j(\omega)}\widehat{\mathcal{W}}^{(l)}_j(\omega, h, Z_{\mathcal{A}})e^{-i\beta'_j(\omega)hZ_{\mathcal{A}}} + \\ (1-\delta_{jj'})\mathbb{E}\left[\mathbb{P}^\varepsilon_{jl}(\omega, Z_{\mathcal{A}}, z)\right]\overline{\mathbb{E}\left[\mathbb{P}^\varepsilon_{j'l'}(\omega, Z_{\mathcal{A}}, z')\right]}e^{Z_{\mathcal{A}}/\mathcal{L}_{jj'}},\end{aligned} \tag{3.24}$$

where the bar denotes complex conjugate, $\widehat{\mathcal{W}}^{(l)}_j$ is the Fourier transform of the mean Wigner distribution described below, and the scale $\mathcal{L}_{jj'}$ is defined in terms of the autocorrelations $\mathcal{R}_\nu$, $\mathcal{R}_{_B}$ and $\mathcal{R}_{_T}$ (see [6, equation (6.26)]). These formulas follow from the calculations in [12, 4] that assume $z = z'$, and the law of iterated expectation with conditioning at z (assuming that $z < z'$). Denoting by $\mathbb{E}_z$ the conditional expectation and using that

$$\mathbb{E}_z\left[\mathbb{P}^\varepsilon_{j'l'}(\omega - \varepsilon^2 h, Z_{\mathcal{A}}, z')\right] \approx \mathbb{P}^\varepsilon_{j'l'}(\omega - \varepsilon^2 h, Z_{\mathcal{A}}, z),$$

because $z' - z$ is much smaller than $O(\varepsilon^{-2})$, we obtain

$$\begin{aligned}\mathbb{E}\left[\mathbb{P}^\varepsilon_{jl}(\omega, Z_{\mathcal{A}}, z)\overline{\mathbb{P}^\varepsilon_{j'l'}(\omega - \varepsilon^2 h, Z_{\mathcal{A}}, z')}\right] &= \mathbb{E}\left[\mathbb{P}^\varepsilon_{jl}(\omega, Z_{\mathcal{A}}, z)\,\mathbb{E}_z\left[\overline{\mathbb{P}^\varepsilon_{j'l'}(\omega - \varepsilon^2 h, Z_{\mathcal{A}}, z')}\right]\right] \\ &\approx \mathbb{E}\left[\mathbb{P}^\varepsilon_{jl}(\omega, Z_{\mathcal{A}}, z)\overline{\mathbb{P}^\varepsilon_{j'l'}(\omega - \varepsilon^2 h, Z_{\mathcal{A}}, z)}\right]\end{aligned}$$

and (3.24) follows from [12, 4] and the fact that $z \ll Z_{\mathcal{A}}/\varepsilon^2$.

The last term in (3.24) corresponds to the coherent part of the mode amplitudes and it is negligible in our regime with $Z_{\mathcal{A}} \gtrsim 3\mathcal{S}_1$. This is by (3.21) and the fact that

$$Z_{\mathcal{A}}\left[\frac{1}{\mathcal{S}_j} + \frac{1}{\mathcal{S}'_j} - \frac{1}{\mathcal{L}_{jj'}}\right] \gtrsim \frac{Z_{\mathcal{A}}}{\mathcal{S}_1} \gtrsim 3.$$

Recalling the expression (3.13) of the mode amplitudes in terms of the propagator, we see that (3.24) states that the amplitudes of different modes are essentially uncorrelated. Therefore, the only second moments that remain large are the mean energies of the modes, which is why we use them in inversion.

3.4. The system of transport equations. The Wigner distribution defines the expectation of the energy of the $j-$th mode resolved over a time window of duration similar to the travel time, when the initial excitation is in the $l-$th mode. It satisfies the following system of transport equations derived in [18, 12, 4]

$$\left[\partial_Z + \beta_j'(\omega)\partial_\tau\right] \mathcal{W}_j^{(l)}(\omega,\tau,Z) = \sum_{q=1}^{N} \Gamma_{jq}^{(c)}(\omega)\mathcal{W}_q^{(l)}(\omega,\tau,Z), \quad Z>0, \tag{3.25}$$

with initial condition

$$\mathcal{W}_j^{(l)}(\omega,\tau,0) = \delta_{jl}\delta(\tau), \tag{3.26}$$

where $\delta(\tau)$ is the Dirac delta distribution. The Fourier transform that appears in (3.24) is defined by

$$\widehat{\mathcal{W}}_j^{(l)}(\omega,h,Z) = \int_{-\infty}^{\infty} d\tau\, \mathcal{W}_j^{(l)}(\omega,\tau,Z)e^{ih\tau}. \tag{3.27}$$

The matrix $\Gamma^{(c)}(\omega)$ in (3.25) models the transfer of energy between the modes, due to scattering. We write it under the assumption that the random processes ν, $\mu_{_B}$ and $\mu_{_T}$ are statistically independent

$$\begin{aligned}\Gamma_{jq}^{(c)}(\omega) =& \frac{\pi^4(jq)^2}{\beta_j(\omega)\beta_q(\omega)X^4}\left[\widehat{\mathcal{R}}_{_B}\left(\beta_j(\omega)-\beta_q(\omega)\right) + \widehat{\mathcal{R}}_{_T}\left(\beta_j(\omega)-\beta_q(\omega)\right)\right] + \\ & \frac{k^4}{4\beta_j(\omega)\beta_q(\omega)}\widehat{\mathcal{R}}_{\nu_{jq}}\left(\beta_j(\omega)-\beta_q(\omega)\right),\end{aligned} \tag{3.28}$$

for $j \neq q$, and

$$\Gamma_{jj}^{(c)}(\omega) = -\sum_{q\neq j}\Gamma_{jq}^{(c)}(\omega), \qquad \forall\, j=1,\dots,N. \tag{3.29}$$

Here $\mathcal{R}_{\nu_{jq}}$ is the autocorrelation of the stationary process

$$\nu_{jq}(z) = \int_0^X dx\, \nu(x,z)\phi_j(x)\phi_q(x), \tag{3.30}$$

and the hat denotes the Fourier transform of the autocorrelations, which is non-negative by Bochner's theorem. Thus $\Gamma_{jq}^{(c)} \geq 0$ for all $j \neq q$, meaning that there is an outflow of energy from mode j to the other modes. The energy lost by this mode is compensated by the gain of energy in the other modes, as stated by relation (3.29).

4. Inversion based on energy transport equations. We now use the results summarized above to formulate our inversion approach. We give in section 4.2 the forward model which maps the source density to the cross-correlations of the mode amplitudes. These are defined in section 4.1 and are self-averaging with respect to different realizations of the random waveguide. Therefore, we can relate them to the mean Wigner distribution. The inversion of the system of transport equations (3.25) is studied in section 4.3, and we explain in section 4.4 what information about the source we can expect to recover.

4.1. Data processing. The first question that arises is how to relate the incoherent array data to the moments $\mathbb{E}\left[\mathbb{P}^{\varepsilon}_{jl}(\omega, Z_{\mathcal{A}}, z)\overline{\mathbb{P}^{\varepsilon}_{jl}(\omega-\varepsilon^2 h, Z_{\mathcal{A}}, z')}\right]$ of the propagator which are defined by the mean Wigner distribution. The answer lies in computing cross-correlations of the data projected on the eigenfunctions ϕ_j, as we now explain.

We denote by $\widehat{D}(\omega, x)$ the Fourier transform of the measurements and by $\widehat{D}_j(\omega)$ its projection on the eigenfunction ϕ_j

$$\widehat{D}_j(\omega) = \int_0^X dx\, \widehat{D}(\omega, x)\phi_j(x). \tag{4.1}$$

We are interested in its cross-correlation $\widehat{\mathcal{C}}_j(h)$ at lag $\varepsilon^2 h$

$$\widehat{\mathcal{C}}_j(h) = \int d\omega\, \widehat{D}_j(\omega)\overline{\widehat{D}_j(\omega-\varepsilon^2 h)}, \tag{4.2}$$

and its inverse Fourier transform

$$\mathcal{C}_j(\tau) = \int_{-\infty}^{\infty} \frac{dh}{2\pi}\, \widehat{\mathcal{C}}_j(h) e^{-ih\tau}. \tag{4.3}$$

The integral in (4.2) is over the bandwidth of the pulse.

We relate below the expectation of $\mathcal{C}_j(\tau)$ to the Wigner distribution, and explain under which conditions $\mathcal{C}_j(\tau)$ is self-averaging, meaning that it is approximately equal to its expectation. The self-averaging is due to the rapid frequency decorrelation of $\widehat{D}_j(\omega)$ over intervals of order $\varepsilon^2\omega_o$, and the bandwidth assumption (3.16). When we divide the bandwidth in intervals of order ε^2/ω_o, we see that in (4.2) we are essentially summing a large number $B/(\varepsilon^2\omega_o) = \varepsilon^{\alpha-2} \gg 1$ of uncorrelated random variables. The self-averaging is basically by the law of large numbers, as long as $\mathbb{E}[\mathcal{C}_j(\tau)]$ is large. This happens for large enough arrays, for long recording times that scale as (3.19), and for properly chosen times τ and centering t_o of the recording window.

The role of the projection (4.1) is to isolate in the data the effect of the $j-$th mode. We see from (3.15)-(3.20) that

$$\widehat{D}_j(\omega) \approx \frac{1}{B}\widehat{f}\left(\frac{\omega-\omega_o}{B}\right)\sum_{q=1}^{N} Q_{jq}\int_{-\infty}^{\infty}\frac{du}{2\pi}\,\widehat{\chi}(u)e^{iu\left[\varepsilon^2 t_o - \beta_q'(\omega_o)Z_{\mathcal{A}}\right]/T}\times$$
$$\int_{\Omega_\rho} d\vec{\mathbf{x}}'\,\rho(\vec{\mathbf{x}}')a_q^+\left(\omega-\frac{\varepsilon^2 u}{T}, \frac{Z_{\mathcal{A}}}{\varepsilon^2}, \vec{\mathbf{x}}'\right)e^{i\left[\beta_q(\omega_o)+(\omega-\omega_o)\beta_q'(\omega_o)\right]\left(\frac{Z_{\mathcal{A}}}{\varepsilon^2}-z'\right)}, \tag{4.4}$$

where we used that the source is supported at ranges that are much smaller than $Z_{\mathcal{A}}/\varepsilon^2$ and introduced the mode coupling matrix $Q \in \mathbb{R}^{N\times N}$ with entries

$$Q_{jq} = \int_0^X dx\, 1_{\mathcal{A}}(x)\phi_j(x)\phi_q(x). \tag{4.5}$$

This coupling is an effect of the aperture of the array. The ideal setup is for an array with full aperture $\mathcal{A} = [0, X]$, because Q is the identity by the orthonormality of the eigenfunctions, and $\widehat{D}_j$ involves only the amplitude of the $j-$th mode. However, all the mode amplitudes enter the expression of $\widehat{D}_j$ when the array has partial aperture, and they are weighted by Q_{jq}. The coupling matrix is diagonally dominant when the length of the aperture $|\mathcal{A}|$ is not much smaller than the waveguide depth X.

This can be seen for example in the case of an array starting at the top boundary $\mathcal{A} = [X - |\mathcal{A}|, X]$, where

$$Q_{jq} = \delta_{jq} - \left(1 - \frac{|\mathcal{A}|}{X}\right) \begin{cases} 1 - \operatorname{sinc}\left(\frac{2\pi j(X-|\mathcal{A}|)}{X}\right), & q = j, \\ \operatorname{sinc}\left(\frac{\pi(j+q)(X-|\mathcal{A}|)}{X}\right) - \operatorname{sinc}\left(\frac{\pi(j-q)(X-|\mathcal{A}|)}{X}\right) & j \neq q. \end{cases} \tag{4.6}$$

We note in (4.4) that by choosing the support of the recording window χ as $\mathcal{T} = \varepsilon^{-2}T$, we can relate $\widehat{D}_j(\omega)$ to the mode amplitudes in a frequency interval of order ε^2. This is important in the calculation of the cross-correlations $\mathcal{C}_j(\tau)$, where the mode amplitudes must be evaluated at nearby frequencies. If we had a smaller $\mathcal{T}$, the cross-correlations would involve amplitude products like $a_q^+\left(\omega, \frac{Z_{\mathcal{A}}}{\varepsilon^2}, \vec{\mathbf{x}}\right)\overline{a_q^+\left(\omega', \frac{Z_{\mathcal{A}}}{\varepsilon^2}, \vec{\mathbf{x}}'\right)}$ for $|\omega - \omega'| \gg \varepsilon^2\omega_o$. These amplitudes are statistically uncorrelated and there is no benefit in calculating the cross-correlation.

We derive in Appendix A the mathematical model of the cross-correlations $\mathcal{C}_j(\tau)$ and obtain that their expectation is given by

$$\mathbb{E}\left[\mathcal{C}_j(\tau)\right] \approx \frac{\|f\|^2}{B}\left|\chi\left(\frac{\tau - \varepsilon^2 t_o}{T}\right)\right|^2 \sum_{q,l=1}^{N} Q_{jq}^2 \frac{\mathcal{W}_q^{(l)}(\omega_o, \tau, Z_{\mathcal{A}})}{4\beta_l(\omega_o)\beta_q(\omega_o)} \left|\widehat{\rho}_l\left[\beta_q(\omega_o)\right]\right|^2, \tag{4.7}$$

where

$$\widehat{\rho}_l(\beta) = \int_{\Omega_\rho} d\vec{\mathbf{x}}\, \rho(\vec{\mathbf{x}})\phi_l(x)e^{-i\beta z} \tag{4.8}$$

are the Fourier coefficients of the unknown source density and

$$\|f\|^2 = \int_{-\infty}^{\infty} du\, |\widehat{f}(u)|^2.$$

We also explain there that $\mathcal{C}_j(\tau)$ is self-averaging (statistically stable) when (4.7) is large. This happens when Q_{jq} is diagonally dominant (i.e., the aperture is large enough), τ is at the peak of the Wigner distribution $\mathcal{W}_j^{(l)}$, and the recording window χ is centered around $\varepsilon^{-2}\tau$.

4.2. The forward model. Because the cross-correlations are self-averaging we can define the forward map $\mathfrak{F}$ from ρ to the vector with entries $\mathcal{C}_j(\tau)$, for $j = 1, \ldots, N$, using equation (4.7). We write it as

$$\left[\mathfrak{F}(\rho)\right]_j(\tau) = \frac{\|f\|^2}{B}\left|\chi\left(\frac{\tau - \varepsilon^2 t_o}{T}\right)\right|^2 \sum_{q,l=1}^{N} Q_{jq}^2 \frac{\mathcal{U}_q^{(l)}(\omega_o, \tau - \beta_q' Z_{\mathcal{A}}, Z_{\mathcal{A}})}{4\beta_l\beta_q} \left|\widehat{\rho}_l\left[\beta_q\right]\right|^2, \tag{4.9}$$

in terms of

$$\begin{aligned} \mathcal{U}_q^{(l)}(\omega_o, \tau, Z_{\mathcal{A}}) &= \mathcal{W}_q^{(l)}(\omega_o, \tau + \beta_q' Z_{\mathcal{A}}, Z_{\mathcal{A}}) \\ &= \int_{-\infty}^{\infty} \frac{dh}{2\pi} e^{-ih\tau}\left(e^{[ih\mathfrak{B}' + \Gamma^{(c)}]Z_{\mathcal{A}}}\right)_{ql} e^{-ih\beta_q' Z_{\mathcal{A}}}, \end{aligned} \tag{4.10}$$

the Wigner transform shifted by the deterministic travel time $\beta_q' Z_{\mathcal{A}}$, and the diagonal matrix

$$\mathfrak{B}' = \operatorname{diag}\left(\beta_1', \ldots, \beta_N'\right). \tag{4.11}$$

We also simplify the notation by dropping the ω_o argument of the wavenumbers β_q, their derivatives β_q' and $\Gamma^{(c)}$. The unknown source density appears in the model as the absolute value of the $N \times N$ matrix of absolute values of its Fourier coefficients (4.8). This is the most that we can expect to recover from the inversion.

If there were no random scattering effects i.e., no matrix $\Gamma^{(c)}$, the right hand-side of (4.10) would equal $\delta_{ql}\delta(\tau)$ and in equation (4.7) we would sum the Dirac delta distributions $\delta\left(\tau - \beta_q' Z_{\mathcal{A}}\right)$ weighted by Q_{jq}^2. In particular, for an array with full aperture where Q equals the identity, the cross-correlation $\mathcal{C}_j(\tau)$ would have a single peak at the travel time $\tau = \beta_j' Z_{\mathcal{A}}$. In the random waveguide the energy of the $j-$th mode is not transported at speed $1/\beta_j'$, because the matrices $\mathfrak{B}'$ and $\Gamma^{(c)}$ in the exponential in (4.10) do not commute. There is anomalous dispersion due to the scattering which must be taken into account in inversion, as explained in the next section.

4.3. Inversion. We have the following unknowns: $Z_{\mathcal{A}}$, the $N \times N$ matrix of absolute values of the Fourier coefficients $\left(|\widehat{\rho}_l(\beta_q)|\right)_{1\leq q,l\leq N}$, and possibly the auto-correlations of the fluctuations. The question is what can be recovered from the cross-correlations $\mathcal{C}_j(\tau)$ and how to carry the inversion.

The range scale $Z_{\mathcal{A}}$ can be determined from the measurements of the travel times τ_j of the energy of the modes, the peaks of $\mathcal{C}_j(\tau)$, using the method introduced in [9, Section 6.1]. It compares τ_j with the travel times predicted by equation (4.7) for a point source at a search range $Z_{\mathcal{A}}^s$ from the array, and estimates $Z_{\mathcal{A}}$ as the range that gives the best fit. Because only the peak times τ_j enter the optimization and not the actual values $\mathcal{C}_j(\tau_j)$, the range estimation is not sensitive to knowing the source density. It works by replacing ρ in (4.9) with the density of a point source at any cross-range in $[0, X]$. Moreover, the search for $Z_{\mathcal{A}}$ can be done in conjunction with the estimation of the autocorrelation of the fluctuations, in case that $\Gamma^{(c)}$ is unknown. The method in [9] has been tested extensively with numerical simulations for both large and small arrays in waveguides with random wave speed. The conclusion is that the estimation of $Z_{\mathcal{A}}$ is very robust, but the success of the estimation of $\mathcal{R}_\nu$ depends on having the right model of the autocorrelation. For example, with a Gaussian model of a Gaussian $\mathcal{R}_\nu$, the optimization determines correctly the correlation length ℓ. For another model the optimization returns the wrong correlation length, but the range $Z_{\mathcal{A}}$ is still well estimated.

To estimate $|\widehat{\rho}_l(\beta_q)|_{1\leq q,l\leq N}$, let us suppose that $Z_{\mathcal{A}}$ has been determined with the method in [9] and that the autocorrelation of the fluctuations i.e., $\Gamma^{(c)}$, is known. This inversion is more delicate than that for $Z_{\mathcal{A}}$ and it cannot succeed without knowing $\Gamma^{(c)}$. Because the time τ does not appear in the ρ dependent factor in (4.9), it suffices to consider the peak values of the cross-correlations $\mathcal{C}_j(\tau_j)$ as the inversion data or alternatively, to integrate $\mathcal{C}_j(\tau)$ over τ. We choose the latter because it is more robust. Assuming that the recording window χ is long enough to contain the essential τ support of $\mathcal{U}_j^{(l)}$ for all $j = 1, \ldots, N$, we define the newly processed data

$$\mathfrak{M}_j := \frac{4B}{\|f\|^2} \int_{-\infty}^{\infty} d\tau\, \mathcal{C}_j(\tau) \approx \sum_{q,l=1}^{N} \frac{Q_{jq}^2}{\beta_l \beta_q} \left(e^{\Gamma^{(c)} Z_{\mathcal{A}}}\right)_{ql} |\widehat{\rho}_l(\beta_q)|^2 , \tag{4.12}$$

and let $\mathfrak{M}$ be the column vector in $\mathbb{R}^N$ with entries (4.12).

Clearly, it is not possible to determine uniquely from the vector $\mathfrak{M}$ the $N \times N$ matrix with entries $|\widehat{\rho}_l(\beta_q)|^2$, unless we have additional assumptions on ρ. To proceed

further, let $\rho(\vec{\mathbf{x}})$ be a separable function

$$\rho(\vec{\mathbf{x}}) = \xi(x)\zeta(z), \tag{4.13}$$

so that

$$\widehat{\rho}_l(\beta) = \widehat{\xi}_l\,\widehat{\zeta}(\beta), \qquad \widehat{\xi}_l = \int_0^X dx\,\xi(x)\phi_l(x), \qquad \widehat{\zeta}(\beta) = \int_{-\infty}^{\infty} dz\,\zeta(z)e^{-i\beta z}. \tag{4.14}$$

Then we can write (4.12) in vector form as

$$\mathfrak{M} \approx \mathbb{Q}\,\mathrm{diag}\left(|\widehat{\zeta}(\beta_1)|^2, \ldots, |\widehat{\zeta}(\beta_N)|^2\right)\mathfrak{B}^{-1}e^{\Gamma^{(c)}Z_{\mathcal{A}}}\mathfrak{B}^{-1}\begin{pmatrix} |\widehat{\xi}_1|^2 \\ \vdots \\ |\widehat{\xi}_N|^2 \end{pmatrix}, \tag{4.15}$$

using matrix $\mathbb{Q}$ with entries Q_{jq}^2 and $\mathfrak{B} = \mathrm{diag}(\beta_1, \ldots, \beta_N)$, and consider two cases:

1. Invert for the range profile $\zeta(z)$ when $\xi(x)$ is known.
2. Invert for the cross-range profile $\xi(x)$ when the source is supported near $z = 0$ in an interval of small length with respect to the wavelength λ_o. Then $\zeta(z)$ is approximately $\delta(z)$ and $\widehat{\zeta}(\beta) \approx 1$.

We analyze both cases under the assumption that $\mathbb{Q}$ is strictly diagonally dominant and therefore invertible. This holds for a large enough aperture $\mathcal{A}$.

Case 1. When we know the cross-range profile $\xi(x)$ of the source we can calculate the Fourier coefficients $\widehat{\xi}_j$, and thus the vector

$$\boldsymbol{\eta} = e^{\Gamma^{(c)}Z_{\mathcal{A}}}\mathfrak{B}^{-1}\begin{pmatrix} |\widehat{\xi}_1|^2 \\ \vdots \\ |\widehat{\xi}_N|^2 \end{pmatrix}. \tag{4.16}$$

Equation (4.15) becomes

$$\mathbb{Q}^{-1}\mathfrak{M} \approx \mathrm{diag}\left(|\widehat{\zeta}(\beta_1)|^2, \ldots, |\widehat{\zeta}(\beta_N)|^2\right)\mathfrak{B}^{-1}\boldsymbol{\eta}, \tag{4.17}$$

and we can invert it as

$$|\widehat{\zeta}(\beta_j)|^2 \approx \frac{\beta_j\left(\mathbb{Q}^{-1}\mathfrak{M}\right)_j}{\eta_j}, \qquad \text{if} \quad \eta_j \neq 0. \tag{4.18}$$

We know that the matrix exponential has a trivial null space, so the vector $\boldsymbol{\eta}$ cannot be zero, but can some of its components be zero or very small?

To answer this question we return to the definition (3.28)-(3.29) of $\Gamma^{(c)}$. This matrix is symmetric, so it has real eigenvalues Λ_j and orthonormal eigenvectors $\mathbf{u}_j$ for $j = 1, \ldots, N$ that form a basis of $\mathbb{R}^N$. The eigenvalues satisfy $\Lambda_j \leq 0$, because otherwise the energy could not be conserved (recall (3.23)), and the null space $\mathrm{Null}(\Gamma^{(c)})$ is nontrivial, because $\mathbf{u}_1 = (1, 1, \ldots, 1)^T/\sqrt{N}$ satisfies $\Gamma^{(c)}\mathbf{u}_1 = \mathbf{0}$ by the definition of $\Gamma^{(c)}$. Let us order the eigenvalues in decreasing order $0 = \Lambda_1 \geq \Lambda_2 \geq \ldots \geq \Lambda_N$, and write the matrix exponential as

$$e^{\Gamma^{(c)}Z_{\mathcal{A}}} = \sum_{j=1}^{N} e^{-|\Lambda_j|Z_{\mathcal{A}}}\,\mathbf{u}_j\mathbf{u}_j^T. \tag{4.19}$$

We can decompose the vector (4.16) in two orthogonal parts: one that lies in $\mathrm{Null}(\Gamma^{(c)})$ and is constant in range, and the other that lies in $\mathbb{R}^N \setminus \mathrm{Null}(\Gamma^{(c)})$ and decays exponentially in range. To be more precise, suppose henceforth that the null space is one dimensional

$$\mathrm{Null}(\Gamma^{(c)}) = \mathrm{span}\{\mathbf{u}_1\}, \tag{4.20}$$

and therefore $\Lambda_2 < 0$. A sufficient (not necessary) condition for this to hold is that all the off-diagonal entries of $\Gamma^{(c)}$ are strictly positive, which happens for typical autocorrelation functions like Gaussians for example. Then $\Gamma^{(c)}$ is a matrix of Perron-Frobenius type, and its largest eigenvalue Λ_1 is simple. Equation (4.16) gives

$$\boldsymbol{\eta} = \mathbf{u}_1 \mathbf{u}_1^T \mathfrak{B}^{-1} \begin{pmatrix} |\widehat{\xi}_1|^2 \\ \vdots \\ |\widehat{\xi}_N|^2 \end{pmatrix} + \boldsymbol{\mathcal{E}} = \frac{1}{N} \left(\sum_{j=1}^{N} \frac{|\widehat{\xi}_j|^2}{\beta_j} \right) \begin{pmatrix} 1 \\ \vdots \\ 1 \end{pmatrix} + \boldsymbol{\mathcal{E}} \tag{4.21}$$

with residual vector $\boldsymbol{\mathcal{E}}$ that decays in range like $\exp(-|\Lambda_2| Z_{\mathcal{A}})$. Thus, all the components of $\boldsymbol{\eta}$ are bounded below by a positive constant as $Z_{\mathcal{A}}$ grows, and the calculation (4.18) is well-posed.

Case 2. Assuming that the source has point-like support in range we let $\widehat{\zeta}(\beta) \approx 1$ in (4.15) and invert the system as

$$\begin{pmatrix} |\widehat{\xi}_1|^2 \\ \vdots \\ |\widehat{\xi}_N|^2 \end{pmatrix} \approx \mathfrak{B}\mathfrak{X} \tag{4.22}$$

where

$$\mathfrak{X} = e^{-\Gamma^{(c)} Z_{\mathcal{A}}} \mathfrak{B}\mathbb{Q}^{-1}\mathfrak{M}. \tag{4.23}$$

However, the calculation of $\mathfrak{X}$ is ill-posed due to the exponential growth in $Z_{\mathcal{A}}$ of the right hand side, so we need regularization. There are many ways to regularize, and the inversion can be improved significantly with prior information about $\xi(x)$. Here we discuss a spectral cut-off regularization which uses the first J terms in the expression (4.19) of the matrix exponential

$$\mathfrak{X}_J = \sum_{j=1}^{J} e^{|\Lambda_j| Z_{\mathcal{A}}} \left(\mathbf{u}_j^T \mathfrak{B}\mathbb{Q}^{-1}\mathfrak{M} \right) \mathbf{u}_j. \tag{4.24}$$

This is the orthogonal projection of $\mathfrak{X}$ on the subspace spanned by the eigenvectors $\{\mathbf{u}_1, \ldots, \mathbf{u}_J\}$ or, equivalently, the minimum Euclidian norm vector that gives a misfit of order $\exp(-|\Lambda_{J+1}| Z_{\mathcal{A}})$ between the data (4.15) and the model.

But in what sense does $\mathfrak{X}_J$ approximate $\mathfrak{X}$ and therefore the vector of absolute values of the Fourier coefficients of ξ? We expect that it should be easier to estimate $|\widehat{\xi}_j|$ for lower indices j that correspond to the fast modes which have less interaction with the random fluctuations than the slow modes. This turns out to be the case, but only if $Z_{\mathcal{A}}$ is not too large.

Recalling (4.22) and the fact that $\mathfrak{B}$ is a diagonal matrix, it is sufficient to investigate if $\mathfrak{X}_J$ approximates better the first components of $\mathfrak{X}$. Let the orthogonal

projector operator be $\mathbb{U}_J$, so that $\mathfrak{X}_J = \mathbb{U}_J \mathfrak{X}$. The error can be bounded as

$$\frac{|(\mathfrak{X} - \mathfrak{X}_J)_j|}{\|\mathfrak{X}\|} = \frac{\|\mathbf{e}_j^T (I - \mathbb{U}_J)\mathfrak{X}\|}{\|\mathfrak{X}\|} \leq \|(I - \mathbb{U}_J)\mathbf{e}_j\| = \sqrt{\sum_{q=J+1}^{N} u_{jq}^2}, \tag{4.25}$$

and it is guaranteed to be small for $1 \leq j \lesssim J$ if the eigenvectors $\mathbf{u}_q$ for $q \geq J+1$ have small entries in the first J rows. Here I is the $N \times N$ identity matrix, $\mathbf{e}_j$ are the vectors of the canonical basis in $\mathbb{R}^N$, and u_{jq} is the entry in the $j-$th row of $\mathbf{u}_q$. We demonstrate next with numerical simulations and with analysis that indeed, the matrix $\mathbf{U} = (\mathbf{u}_1, \ldots, \mathbf{u}_N)$ of eigenvectors of $\Gamma^{(c)}$ has a nearly vanishing block in the upper right corner.

• **Numerical simulations:** We consider a waveguide with flat boundaries and random wave speed with Gaussian autocorrelation of the fluctuations ν

$$\mathcal{R}_\nu(x, x', z) = \mathbb{E}\left[\nu(x, z)\nu(x', z)\right] = e^{-\frac{(x-x')^2}{2\ell^2} - \frac{z^2}{2\ell^2}}. \tag{4.26}$$

This is a good setup because, as we explain in section 5 (see also [8]), the transport based inversion method is most useful in waveguides where the fluctuations of the wave speed dominate those of the boundaries. Using (4.26) in the definition (3.28)-(3.29) of $\Gamma^{(c)}$, we obtain that

$$\Gamma^{(c)}_{jq} \approx \frac{\pi}{X} \frac{\ell^2 k_o^4}{\beta_j \beta_q} e^{-\frac{1}{2}\ell^2(\beta_j - \beta_q)^2} \left[e^{-\frac{(k_o \ell)^2}{2}\frac{(j-q)^2}{N^2}} + e^{-\frac{(k_o \ell)^2}{2}\frac{(j+q)^2}{N^2}} \right], \qquad j \neq q, \tag{4.27}$$

where $k_o = \omega_o / c_o$, and the approximation is for $\ell \ll X$.

We take $c_o = 1.5$km/s, the sound speed in water, the wavelength $\lambda_o = 1.5$m corresponding to central frequency 1kHz, $X = 20.3\lambda_o$, so that $N = 40$, and three choices of the correlation length: $\ell = \lambda_o$, $\ell = 3\lambda_o$ and $\ell = 5\lambda_o$. We display in the left plots of Figure 4.1 the absolute values of the entries in the matrix $\mathbf{U}$ of the eigenvectors, and in the right plots the scattering mean free paths of the modes and the range scales $1/|\Lambda_j|$, for $j = 2, \ldots, N$. These scales should be multiplied by ε^{-2}, so for example in media with 1% fluctuations, the ordinate is in units of $\times 10^4$m.

The left plots in Figure 4.1 show that there is an index $j_\star$ such that the first entries of the eigenvectors $\mathbf{u}_j$ are negligible for $j > j_\star$. In the first simulation $j_\star \approx 5$, in the second $j_\star \approx 15$ and in the last $j_\star \approx 25$. Thus, if $Z_{\mathcal{A}}$ is not too large, we can expect from the error estimate (4.25) that $\mathfrak{X}_{j_\star}$ gives a good approximation of the first components of $\mathfrak{X}$. The right plots in Figure 4.1 show that $1/|\Lambda_{j_\star}| \approx \mathcal{S}_1$, so the cutoff at $J = j_\star$ can be used when the waves are barely incoherent (i.e., for $Z_{\mathcal{A}} \gtrsim \mathcal{S}_1$). For larger $Z_{\mathcal{A}}$ we must reduce J to stabilize the inversion, and obtain less accurate results. When $Z_{\mathcal{A}}$ is really large, satisfying $Z_{\mathcal{A}} \gg \mathcal{L}_{eq}$, where

$$\mathcal{L}_{eq} = 1/|\Lambda_2|$$

is known as the equipartition distance, we must take $J = 1$ and thus obtain no information about the source. The equipartition distance is the range scale on which the mean energies become uniformly distributed over the modes. The cumulative scattering is so strong at such ranges that the waves forget their initial state, they are independent of the cross-range profile of the source.

• **Analysis:** Here we use a simplified model Υ of $\Gamma^{(c)}$ to show with analysis that $\mathbf{U}$ has a nearly vanishing block in the upper right corner. The model neglects the

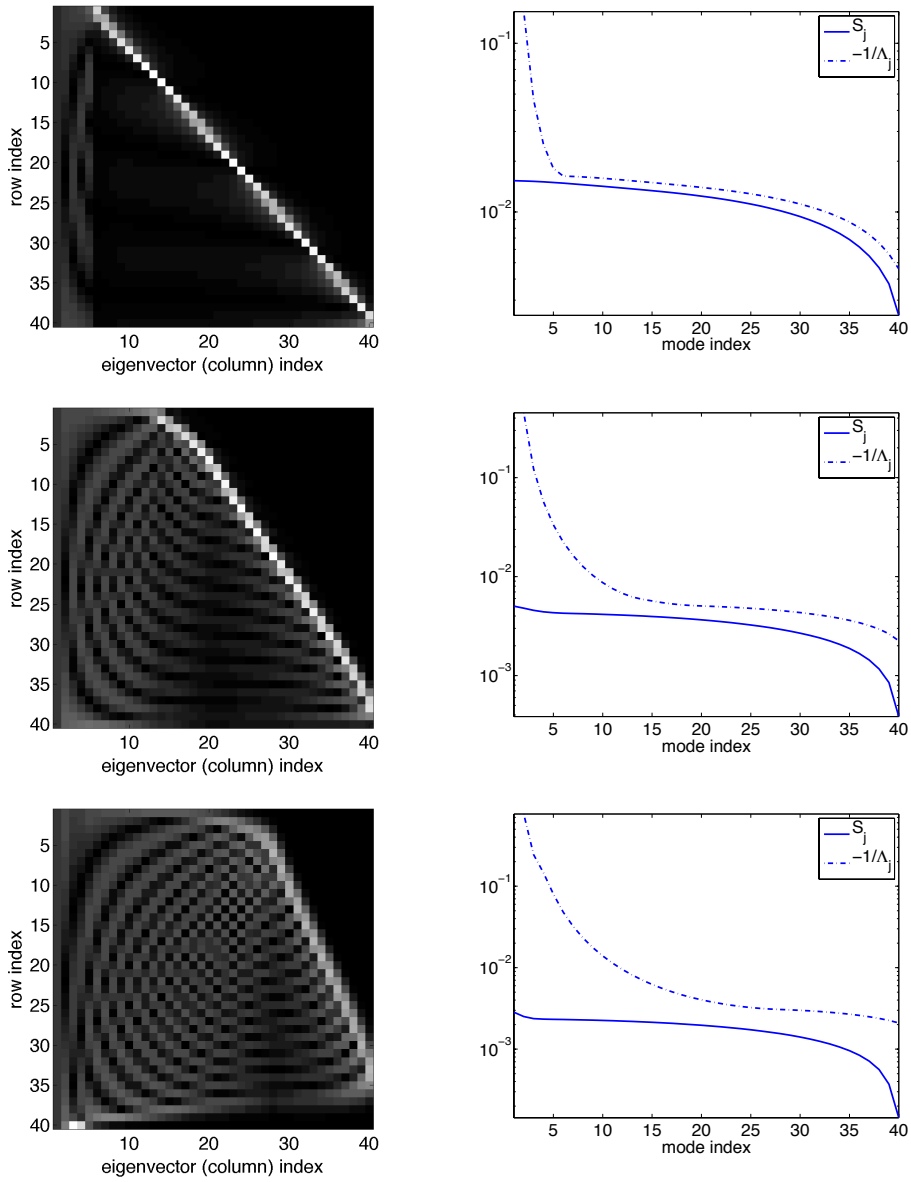

FIG. 4.1. *Left plots: Absolute values of the entries of the matrix* $\mathbf{U}$ *of eigenvectors. Gray scale with lighter color indicates larger values and black indicates nearly zero. The column index is in the abscissa and the row index in the ordinate. Right plots: The scattering mean free path of the modes (full line) and the scales* $-1/\Lambda_j$*, for* $j = 2, \ldots N$ *(dotted line). In the top row* $\ell = \lambda_o$*, in the middle row* $\ell = 3\lambda_o$ *and in the last row* $\ell = 5\lambda_o$*.*

energy transfer between modes that are not immediate neighbors, meaning that Υ is tridiagonal. It applies to a different regime than that considered in the numerical simulations, so the results complement the previous ones. The regime is for large correlation lengths satisfying

$$k_o \ell = O(N), \qquad N \gg 1,$$

so that Υ is a good approximation (up to a multiplicative factor) of $\Gamma^{(c)}$.

The definition of Υ is

$$k_o \Upsilon_{jq} = \begin{cases} \Gamma^{(c)}_{jq}, & |j-q| = 1, \\ 0, & |j-q| > 1, \end{cases} \tag{4.28}$$

for $j \neq q$, and

$$k_o \Upsilon_{jj} = \begin{cases} -\Gamma^{(c)}_{jj-1} - \Gamma^{(c)}_{jj+1}, & 2 \leq j \leq N-1, \\ -\Gamma^{(c)}_{12}, & j = 1, \\ -\Gamma^{(c)}_{N-1N}, & j = N. \end{cases} \tag{4.29}$$

We factor out k_o for convenience of the calculations, and use the expression (3.28) of $\Gamma^{(c)}$ with the assumption that the fluctuations in the medium play the dominant role. Then, the diagonal of Υ scales as

$$\Upsilon_{jj} \sim \frac{N^2}{N-j+1}, \qquad j = 1, \ldots, N. \tag{4.30}$$

We summarize the properties of the spectrum of Υ in the next proposition proved in appendix B. We denote its eigenvectors and eigenvalues with the same symbols $\mathbf{u}_j$ and Λ_j. This is an abuse of notation, but the spectrum of $\Gamma^{(c)}$ can be related to that of Υ using known perturbation theory [21].

PROPOSITION 4.1. *The tridiagonal matrix Υ has the following properties:*

1. *The eigenvectors form an orthonormal basis of $\mathbb{R}^N$ and $\Lambda_j \leq 0$.*
2. *The null space is one dimensional.*
3. *The norm is $\|\Upsilon\| = O(N^2)$.*
4. *$|\Lambda_j| = O(N^2)$ for indices j satisfying $N - j = O(1)$.*
5. *If Λ_j is a "large eigenvalue", meaning that $\delta = N/|\Lambda_j| \ll 1$, and J is a spectral cut-off satisfying $J \leq N/2$, we have $\sum_{q=1}^{J} u_{qj}^2 \leq O(\delta^2)$.*

The first two properties are the same as those stated earlier for $\Gamma^{(c)}$, under the assumption that its off-diagonal entries are strictly positive. The last property confirms our expectation that the matrix $\mathbf{U}$ of the eigenvectors has a nearly vanishing upper right corner.

4.4. Source estimation. We have now seen that we can only expect to determine the absolute value of a few Fourier coefficients of $\rho(\vec{\mathbf{x}})$. Thus, it is impossible to estimate in detail a general source density, unless we restrict the search to a specific class of functions. Here are a few examples:

• **Point like source.** If we let $\rho(\vec{\mathbf{x}}) = \delta(x - x_\star)\delta(z)$, it is enough to determine the absolute value of the first Fourier coefficient

$$|\widehat{\rho}_1(\beta)| \approx |\phi_1(x_\star)|, \qquad \forall \beta.$$

Since $|\phi(x)|$ is monotonically increasing for $x \in [0, X/2)$ and decreasing for $x \in (X/2, 0]$, this gives the cross-range location $x_\star$ up to a reflection with respect to the axis of the waveguide. This reflection ambiguity cannot be resolved by estimating higher order Fourier coefficients of ρ. It is due to the symmetric boundary conditions at $x = 0$ and $x = X$. If we had Dirichlet conditions at $x = X$ and Neumann at $x = 0$,

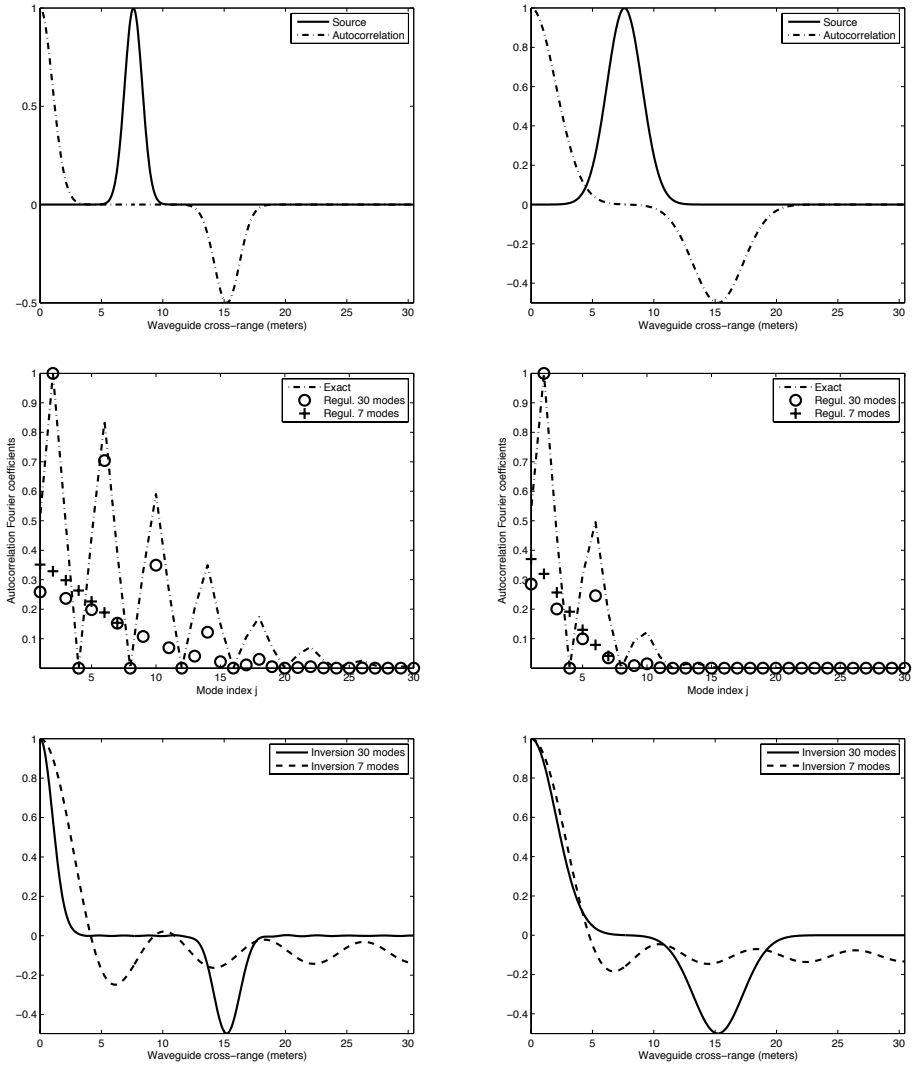

FIG. 4.2. *Left plots* $\xi(x) = \mathcal{N}(x_o = X/4, \sigma = X/30)$. *Right plots* $\xi(x) = \mathcal{N}(x_o = X/4, \sigma = X/15)$. *Top line the source cross-range profile* $\xi(x)$ *(full line) and the autocorrelation* $\mathcal{R}_\xi(x)$ *(dotted line). Middle plots show the exact* $|\xi_j|^2$ *and the recovered ones for cut-off at* $J = 30$ *(circle) and* $J = 7$ *(cross). Bottom plots display the recovered autocorrelation for cut-off at* $J = 30$ *(full line) and* $J = 7$ *(dotted line).*

$|\phi_1(x)|$ would be monotone in $(0, X)$ and $x_\star$ would be uniquely determined by $|\widehat{\rho}_1(\beta)|$. We discuss next a more robust way of estimating the support of the source.

• **Size of cross-range support.** Let us denote by $\xi_e(x)$ the odd extension of the cross-range profile of the source about $x = 0$, and define its autocorrelation

$$\mathfrak{R}_\xi(x) = \int_{-X}^{X} dx'\, \xi_e(x')\xi_e(x'+x) = 2\sum_{j=1}^{\infty} |\widehat{\xi}_j|^2 \cos\left(\frac{\pi j x}{X}\right), \tag{4.31}$$

where the last equality follows by direct calculation using the Fourier sin series ex-

pansion of the real valued $\xi_e(x)$. Obviously, we can approximate $\mathfrak{R}_\xi(x)$ using the regularized solution described in Case 2 of the previous section, if the Fourier coefficients $\widehat{\xi}_j$ are small for $j > J$. Otherwise, we get the autocorrelation of a smoothed version of the source. To illustrate what we can expect, suppose that $\xi(x) = \mathcal{N}(x - x_o, \sigma)$, where

$$\mathcal{N}(x;\sigma) = \tfrac{1}{\sqrt{2\pi}\,\sigma} e^{-\frac{x^2}{2\sigma^2}}$$

is the normalized Gaussian centered at x_o, with standard deviation σ. We assume that $\sigma \ll X$ and that the essential support of the Gaussian is inside the interval $(0, X)$. The odd extension is $\xi_e(x) = \mathcal{N}(x - x_o, \sigma) - \mathcal{N}(x + x_o, \sigma)$, and the autocorrelation is given by

$$\mathfrak{R}_\xi(x) \approx 2\,\mathcal{N}(x; \sqrt{2}\,\sigma) - \mathcal{N}(x - 2x_o; \sqrt{2}\,\sigma) - \mathcal{N}(x + 2x_o; \sqrt{2}\,\sigma). \tag{4.32}$$

The first right term in (4.32) is invariant to translations of the source, and can be used to estimate the cross-range support of the source (i.e., σ). The remaining two terms depend on the source location, and can be used to estimate x_o. Because the autocorrelation is a $2X$-periodic function, the translation by $2x_o$ in (4.32) is understood modulo $2X$. Consequently, sources that are symmetrically located about the center of the waveguide ($x = X/2$) produce the same autocorrelation. That is to say, the location x_m of the minimum of the autocorrelation determines the center of the source up to a reflection ambiguity: at $x_o = x_m/2$ or at its reflection $x_o = X - x_m/2$.

In Figure 4.2 we present inversion results for $\xi(x) = \mathcal{N}(X/4, X/30)$ (left plots) and $\xi(x) = \mathcal{N}(X/4, X/15)$ (right plots). The plots on the top line show the source cross-range profile and the autocorrelation $\mathcal{R}_\xi(x)$. The plots in the middle line show the exact values $|\widehat{\xi}_j|^2$ and the estimated ones for cut-off at $J = 30$ and $J = 7$, respectively. The estimates are calculated using (4.22) with regularization (4.24). For the cut-off at $J = 30$ the array is at $Z_{\mathcal{A}} = \mathcal{L}_{eq}/40$, and for $J = 7$ we have $Z_{\mathcal{A}} = \mathcal{L}_{eq}/10$. The regularization is chosen so that the exponentials in (4.24) are bounded by

$$e^{|\Lambda_j| Z_{\mathcal{A}}} \lesssim 10, \quad j = 1, \ldots, J.$$

The bottom plots show the estimated autocorrelation calculated using equation (4.31), with the series truncated at $j = J$ and $|\widehat{\xi}_j|^2$ replaced by the estimates. The results show that the regularization with $J = 30$ gives a good approximation of the (first) largest Fourier coefficients and therefore of the autocorrelation. However, the estimates for $J = 7$ are poor and give no information about the location of the source (the minimum of the autocorrelation is not evident in the estimates). The standard deviation of the Gaussian centered at zero (the peak of the autocorrelation), which determines the width of the support of the source, is related to the rate of decay of the Fourier coefficients. Thus, we can estimate it even for $J = 7$ in the case of the broader source (bottom right plot) but not for the narrower source (bottom left plot).

• **Size of range support.** The autocorrelation of the range profile is

$$\mathfrak{R}_\zeta(z) = \int_{-\infty}^{\infty} dz'\, \zeta(z')\zeta(z'+z) = \frac{1}{\pi}\int_0^{\infty} d\beta\, |\widehat{\zeta}(\beta)|^2 \cos(\beta z),$$

where we used that $\zeta(z)$ is real valued. We can approximate $\mathfrak{R}_\zeta$ from $\{|\widehat{\zeta}(\beta_j)|\}_{1\le j\le N}$ when $N \gg 1$, so that β_j sample well the interval $(0, k)$, and $|\widehat{\zeta}(\beta)| \ll 1$ for $\beta > \beta_1 \approx k$. We already know that the source is centered at $z = 0$, and the size of the support of $\zeta(z)$ follows from that of $\mathfrak{R}_\zeta(z)$ as above.

5. Summary and discussion. We presented an analysis of the inverse source problem in perturbed two dimensional acoustic waveguides, with data given by time resolved measurements of the pressure field $p(t, \vec{\mathbf{x}})$ at a remote array of sensors. The waves are trapped by pressure release boundaries and are guided along the the range direction, the axis of the waveguide. The perturbations consist of small scale fluctuations of the boundaries and the sound speed in the medium that fills the waveguide. Such fluctuations cannot be known in detail in practice and are thus modeled with random processes. This places the problem in a stochastic framework. The inversion is carried in a single waveguide, one realization of the random model, and the goal is to obtain robust estimates of the source density $\rho(\vec{\mathbf{x}})$. Robust means insensitive (statistically stable) with respect to the particular realization of the random perturbations of the waveguide.

Typical imaging methods are based on the assumption that the field $p(t, \vec{\mathbf{x}})$ is coherent, equal to its statistical expectation plus some small additive noise. This holds approximately in weak scattering regimes i.e., when the array is not too far from the source. We consider strong scattering regimes where $p(t, \vec{\mathbf{x}})$ is incoherent, it is essentially a random, mean zero field.

Our inversion methodology is based on the theory of wave propagation in random waveguides [18, 10, 12, 13, 4]. This theory decomposes the wave field in a countable set of modes, which are time harmonic propagating and evanescent waves. It models the cumulative wave scattering effects of the perturbations in the waveguide by the mode amplitudes, which are complex valued random fields. We use their statistical description to obtain the following results: (1) We show how to get high fidelity estimates of the energy carried by the modes to the array from cross-correlations of the incoherent data. We explain which cross-correlations are useful and how to calculate them. (2) As the waves propagate and scatter in the random waveguide, they interchange energy. This is described by a system of transport equations with initial condition that depends on the unknown source density ρ. We analyze the invertibility of this system. (3) We quantify what can be recovered about the source in terms of the range to the array. The cumulative scattering effects impede the inversion process, and the longer the range, the more pronounced the impediment.

The energies of the propagating modes encode the source information in terms of a matrix of absolute values of Fourier coefficients of ρ. It is impossible to determine this matrix uniquely from the estimated energies (the problem is under-determined), unless there is additional information about ρ. We assume that it is a separable function $\rho(\vec{\mathbf{x}}) = \xi(x)\zeta(z)$, where x is the cross-range component of $\vec{\mathbf{x}}$ and z is the range, along the axis of the waveguide. We study in detail two cases: (1) The estimation of the range profile $\zeta(z)$ when the cross-range $\xi(x)$ is known, and (2) The estimation of the cross-range profile $\xi(x)$ when the source has point-like support in range $\zeta(z) = \delta(z)$. Other known range profiles $\zeta(z)$ may be considered as well, but they do not bring new insight to the inversion process. In both cases there is ambiguity about the source, because only the absolute value of the Fourier coefficients of $\zeta(z)$ or $\xi(x)$ can be determined. We can expect only limited information about $\rho(\vec{\mathbf{x}})$, such as the size of its support in range or cross-range. This can be estimated from the autocorrelation functions of $\zeta(z)$ or $\xi(x)$, which can be approximated using the absolute values of their Fourier coefficients.

The range profile estimation turns out to be the easier of the two cases. We can determine the vector $(|\widehat{\zeta}(\beta_j)|)_{1\leq j\leq N}$ of absolute values of the Fourier transform of $\zeta(z)$ evaluated at the wavenumbers β_j of the N propagating modes, and the calculation is

well posed no matter how far the array is from the source. The wavenumbers β_j sample the interval $(0, \omega_o/c_o)$, in steps that decrease monotonically with N. Here ω_o is the central frequency of the signal emitted by the source and c_o is the reference wave speed in the medium that fills the waveguide. Thus, we can obtain good approximations of the autocorrelation of the range profile $\zeta(z)$, specially in high frequency regimes.

The cross-range estimation entails the calculation of the vector $(|\widehat{\xi}_j|)_{1\le j\le N}$ of Fourier coefficients of $\xi(x)$. The Fourier basis is defined by the eigenfunctions of the second derivative operator in x, which are sin functions in our case. Although the mode energies define uniquely the vector $(|\widehat{\xi}_j|)_{1\le j\le N}$, the calculation is ill posed and the problem becomes worse as the range separation between the source and the array increases. Cumulative scattering transfers energy between the modes, and the longer the waves travel, the harder it is to determine the initial energy distribution, which is defined by $(|\widehat{\xi}_j|)_{q\le j\le N}$. There is a range scale, called the equipartition distance $\mathcal{L}_{eq}$, beyond which the energy becomes uniformly distributed between the modes, independent of the initial state. The waves lose all information about the cross-range profile at such ranges, and the inversion for $\xi(x)$ becomes impossible.

The interesting regime for the estimation of $\xi(x)$ is for ranges between the scattering mean free path $\mathcal{S}_1$ of the fastest propagating mode and $\mathcal{L}_{eq}$. The scattering mean free paths are mode dependent range scales at which the mode amplitudes become incoherent, meaning that they are essentially mean zero random fields. These scales are longer for the faster modes which travel along more direct trajectories from the source to the array. The slow modes spend a longer time in the waveguide because they reflect many times at the boundaries. They have more opportunity to interact with the perturbations and thus lose their coherence on shorter range scales.

The mode dependence of the scattering mean free paths is much more pronounced when the boundary fluctuations are stronger than those of the sound speed [4, 8], and $\mathcal{S}_1 \approx \mathcal{L}_{eq}$. The transport based inversion described in this paper is not useful for estimating the cross-range profile of the source in such waveguides. For ranges that are smaller than $\mathcal{S}_1$, the waves are partially coherent and it is easier and better to estimate the source with coherent methods complemented with data processing that filters out the incoherent modes, as shown in [8]. For ranges that exceed $\mathcal{S}_1 \approx \mathcal{L}_{eq}$ the estimation of the cross-range is impossible, because the waves are in the equipartition regime. However, the range profile of the source can be estimated as described in this paper, even for ranges that exceed $\mathcal{L}_{eq}$.

The mode dependence of the scattering mean free paths is not so strong when the scattering in the medium dominates. Moreover, there is a gap between $\mathcal{L}_{eq}$ and $\mathcal{S}_1$, as illustrated in Figure 4.1. Our transport based inversion is useful for estimating the support of the cross-range profile of $\rho(\vec{\mathbf{x}})$, at ranges that fall in this gap.

The analysis in this paper is for two dimensional waveguides with reflecting boundaries. It extends to leaky waveguides where energy is lost by radiation through a boundary, such as the ocean floor. The system of transport equations that models the propagation of energy in such waveguides is derived in [18, Equation (4.3)]. It is almost the same as the system analyzed in this paper, expect that there is damping of energy due to the radiation. This damping adds to the ill posedness of the inverse problem.

Extensions to three dimensional acoustic waveguides with reflecting boundaries are straightforward, and do not introduce anything new if there are no degeneracies (multiplicity) of the eigenvalues of the Laplacian in the cross-range. It is difficult to quantify such degeneracies for arbitrary cross-sections of the waveguide. But in

certain cases like rectangular cross-sections with sides L_1 and L_2, degeneracies occur if and only if L_1/L_2 is a rational number. In vectorial problems, such as electromagnetic waveguides, degeneracies are unavoidable for any cross-range profile, because of different states of polarization of the waves [3, 20]. Degeneracies are interesting because they introduce statistical correlations between the amplitudes of the modes that correspond to degenerate eigenvalues. We no longer have scalar valued energies carried by each mode, but Hermitian matrices that describe the propagation of energy by the set of degenerate modes [3]. The transport equations are more complicated [3], but they may lead to extra information about the cross-range profile of the source, not just the absolute value of its Fourier coefficients. However, there is no gain in the stability of the inverse problem. The transfer of energy between the modes occurs in any type of random waveguide, and the estimation of the initial energy state, which determines the cross-range of the source, remains exponentially ill-posed.

Acknowledgements. The work of S. Acosta, R. Alonso and L. Borcea was partially supported by the AFOSR Grant FA9550-12-1-0117, the ONR Grant N00014-12-1-0256.

Appendix A. The model of the cross-correlations.

We obtain from (4.3), (4.4) and definition (3.13) that relates the mode amplitudes to the propagator that

$$\begin{aligned}\mathcal{C}_j(\tau) \approx \int_{-\infty}^{\infty} \frac{d\omega}{B^2} \left|\widehat{f}\left(\frac{\omega-\omega_o}{B}\right)\right|^2 \sum_{q,q'=1}^{N} Q_{jq}Q_{jq'} \sum_{l,l'=1}^{N} \frac{\widehat{\rho}_l[\beta_q(\omega)]\,\overline{\widehat{\rho}_{l'}}[\beta_{q'}(\omega)]}{4\beta_l(\omega_o)\beta_{l'}(\omega_o)} \times \\ \int_{-\infty}^{\infty} \frac{du}{2\pi}\,\widehat{\chi}(u) e^{iu\left[\varepsilon^2 t_o - \beta'_q(\omega_o) Z_{\mathcal{A}}\right]/T} \int_{-\infty}^{\infty} \frac{du'}{2\pi}\,\overline{\widehat{\chi}(u')} e^{-iu'\left[\varepsilon^2 t_o - \beta'_{q'}(\omega_o) Z_{\mathcal{A}}\right]/T} \times \\ e^{i\frac{Z_{\mathcal{A}}}{\varepsilon^2}\left\{\beta_q(\omega_o)-\beta_{q'}(\omega_o)+(\omega-\omega_o)[\beta'_q(\omega_o)-\beta'_{q'}(\omega_o)]\right\}} \int_{-\infty}^{\infty} \frac{dh}{2\pi}\, e^{-ih\left[\tau-\beta'_{q'}(\omega_o) Z_{\mathcal{A}}\right]} \times \\ \mathbb{P}^{\varepsilon}_{ql}\left(\omega - \frac{\varepsilon^2 u}{T}, Z_{\mathcal{A}}, z'\right) \overline{\mathbb{P}^{\varepsilon}_{q'l'}\left(\omega - \varepsilon^2 h - \frac{\varepsilon^2 u'}{T}, Z_{\mathcal{A}}, z'\right)}, \end{aligned} \tag{A.1}$$

where $\widehat{\rho}_k(\beta)$ are the Fourier coefficients of the source density defined by (4.8).

When we calculate the expectation of (A.1) using the moment formula (3.24), we see that only the terms with $q = q'$ and $l = l'$ survive in the sum. The coherent terms for $q = l$, $q' = l'$ and $q \neq q'$ in the second moment (3.24) do not appear at full aperture, where $Q_{jq} = \delta_{jq}$. It the array has partial aperture but $\mathcal{A}$ is large enough to have a diagonally dominant matrix Q, the coherent terms are small because of the small weights Q_{jq} for $q \neq j$, and specially because of the assumption that $Z_{\mathcal{A}} \gtrsim 3\mathcal{S}_1$. The result is

$$\begin{aligned}\mathbb{E}\left[\mathcal{C}_j(\tau)\right] \approx \int_{-\infty}^{\infty} \frac{d\omega}{B^2} \left|\widehat{f}\left(\frac{\omega-\omega_o}{B}\right)\right|^2 \sum_{q=1}^{N} Q_{jq}^2 \sum_{l=1}^{N} \frac{\left|\widehat{\rho}_l\left[\beta_q(\omega)\right]\right|^2}{4\beta_l(\omega_o)\beta_q(\omega_o)} \times \\ \int_{-\infty}^{\infty} \frac{du}{2\pi}\,\widehat{\chi}(u) e^{iu\varepsilon^2 t_o/T} \int_{-\infty}^{\infty} \frac{du'}{2\pi}\,\overline{\widehat{\chi}(u')} e^{-iu'\varepsilon^2 t_o/T} \times \\ \int_{-\infty}^{\infty} \frac{dh}{2\pi}\, e^{-ih\tau} \widehat{\mathcal{W}}_q^{(l)}\left(\omega, h + (u'-u)/T, Z_{\mathcal{A}}\right), \end{aligned} \tag{A.2}$$

where we note that the last integral is the inverse Fourier transform of the mean Wigner distribution. Equation (4.7) follows after using that the bandwidth is small

and that $\mathcal{W}_q^{(l)}$ varies smoothly with respect to the first argument. We also use that the Fourier transform $\widehat{\rho}_l(\beta)$ is smooth in β. In fact it is analytic because ρ has compact support.

To assess the statistical stability of $\mathcal{C}_j(\tau)$, we need the fourth order moments of the propagator. These are given in [9, Appendix D], and the estimate of the variance of $\mathcal{C}_j(\tau)$ follows after a long calculation which we explain briefly. Since the variance is

$$\mathrm{var}\left[\mathcal{C}_j(\tau)\right] = \mathbb{E}\left[\left|\mathcal{C}_j(\tau)\right|^2\right] - \left|\mathbb{E}\left[\mathcal{C}_j(\tau)\right]\right|^2,$$

we need fourth order moments like

$$\mathbb{E}\left[\mathbb{P}^{\varepsilon}_{q_1 l_1}\left(\omega, Z_{\mathcal{A}}, z_1\right)\overline{\mathbb{P}^{\varepsilon}_{q_2 l_2}\left(\omega, Z_{\mathcal{A}}, z_2\right)}\mathbb{P}^{\varepsilon}_{q_1' l_1'}\left(\omega', Z_{\mathcal{A}}, z_1'\right)\overline{\mathbb{P}^{\varepsilon}_{q_2' l_2'}\left(\omega', Z_{\mathcal{A}}, z_2'\right)}\right]$$

where we neglect the order ε^2 offsets in the arguments, because they do not play any role. These moments factorize in the product of two second moments at frequencies ω and ω' when $|\omega' - \omega| \gg \varepsilon^2\omega_o$, so in the calculation of the variance we are left with the integration over the small strip $\{\omega, \omega' : \ |\omega - \omega'| \ll \varepsilon^2\omega_o\}$. This makes the variance smaller than the square of the mean (4.7), by a factor of $\varepsilon^2\omega_o/B = \varepsilon^{2-\alpha} \ll 1$, as long as the mean is large. This happens for example when the matrix Q is diagonally dominant and we evaluate the cross-correlation at a time τ for which $\mathcal{W}_j^{(l)}$ is large.

Appendix B. Proof of Proposition 4.1. That the eigenvectors form an orthonormal basis follows from the symmetry of Υ. We also obtain from (4.28)-(4.29) that the quadratic forms of Υ are

$$\mathbf{v}^T\Upsilon\mathbf{v} = -\sum_{j=2}^{N}\Upsilon_{jj-1}\left(v_j - v_{j-1}\right)^2 \leq 0, \qquad \forall\ \mathbf{v} = (v_1, \ldots, v_N)^T \in \mathbb{R}^N,$$

so the eigenvalues must satisfy $\Lambda_j \leq 0$. We order them as $0 = \Lambda_1 \geq \Lambda_2 \geq \ldots \Lambda_N$.

We have $(1, 1, \ldots, 1)^T \in \mathrm{Null}(\Upsilon)$ by construction. To prove property 2, we take a large enough γ so that all the entries in the matrix

$$\Upsilon_{\gamma} = \Upsilon + \gamma I$$

are positive. This matrix is of Perron-Frobenius type, and its eigenvalues are equal to $\Lambda_j + \gamma$. The largest eigenvalue $\Lambda_o + \gamma$ is simple, and therefore the null space of Υ is one dimensional.

The variational definition of $|\Lambda_N|$ as the maximum of the Rayleigh quotient of $-\Upsilon$ gives that $|\Lambda_N|$ is larger than $|\Upsilon_{jj}|$, for any $j = 1, \ldots, N$. But $\Upsilon_{NN} = O(N^2)$ by (4.30), and property 3 follows from $\|\Upsilon\| = |\Lambda_N|$.

Consider square blocks Υ_m of Υ, containing the last $m = O(1)$ elements on its diagonal. By (4.30) they scale like

$$\Upsilon_m = N^2\widetilde{\Upsilon}_m,$$

where $\widetilde{\Upsilon}_m$ have entries of order one. Cauchy's interlacing theorem gives that

$$|\Lambda_{N-m+j}| \geq N^2|\widetilde{\lambda}_j|, \quad j = 1, \ldots, m,$$

where $\widetilde{\lambda}_j \leq 0$ are the eigenvalues of $\widetilde{\Upsilon}_m$ in decreasing order. To prove Property 4 it remains to show that these are all $O(1)$. First, let us see that $\widetilde{\Upsilon}_m$ has a trivial null space. Indeed, suppose that $\mathbf{v} \in \text{Null}(\widetilde{\Upsilon}_m)$ and write equation

$$\widetilde{\Upsilon}_m \mathbf{v} = \mathbf{0}$$

row by row. Starting from the last row to the second, and using definitions (4.28)-(4.29), we obtain that all entries in $\mathbf{v}$ must be equal to say v. However, the first equation gives that $v = 0$, because the elements in the first row of $\widetilde{\Upsilon}_m$ do not add to zero. Thus, the null space is trivial. The smallest in magnitude eigenvalue equals the minimum of the Rayleigh quotient

$$\frac{\mathbf{v}^T(-\widetilde{\Upsilon}_m)\mathbf{v}}{\mathbf{v}^T\mathbf{v}} = \left[\widetilde{\beta}_{N-m} v_1^2 + \sum_{j=1}^{m-1} \widetilde{\beta}_{N-m+j}(v_{j+1} - v_j)^2\right] / \sum_{j=1}^{N} v_j^2,$$

where $\widetilde{\beta}_j = \beta_j / N^2 = O(1)$ and the right hand side is obtained by direct calculation. All the terms in this expression are non-negative and at least one of them must be $O(1)$. Thus, we see that $|\widetilde{\lambda}_j| \geq O(1)$ and property 4 follows.

To prove the last property, let Λ be a large eigenvalue of Υ and $\mathbf{u}$ its associated eigenvector. We see from definition (4.28)-(4.29) that $|\Upsilon_{jj}| \geq \Upsilon_{jj\pm1}$, and using that

$$|\Lambda| u_j = -\Upsilon_{jj-1} u_{j-1} + |\Upsilon_{jj}| u_j - \Upsilon_{jj+1} u_{j+1},$$

we obtain the bound

$$|\Upsilon_{jj}| \left(|u_{j-1}| + |u_j| + |u_{j+1}|\right) \geq |\Lambda| |u_j|.$$

Moreover, multiplying by $|u_j|$ and summing over $j = 2, \ldots, J$ we get the estimate

$$\begin{aligned}\sum_{j=2}^{J} u_j^2 &\leq |\Lambda|^{-1} \sum_{j=2}^{J} |\Upsilon_{jj}| \left(|u_{j-1} u_j| + u_j^2 + |u_{j+1} u_j|\right) \\ &\leq \frac{C\delta N}{N+1-J} \sum_{j=2}^{J} \left(|u_{j-1} u_j| + u_j^2 + |u_{j+1} u_j|\right),\end{aligned}$$

with the second inequality implied by (4.30) and $1/|\Lambda| = \delta/N$. Since $J \leq N/2$, we have $N/(N+1-J) \leq 2$. Now use Young's inequality

$$|u_j u_{j\pm1}| \leq \frac{\widetilde{\delta} u_{j\pm1}^2}{2} + \frac{u_j^2}{2\widetilde{\delta}},$$

which holds for any $\widetilde{\delta} > 0$. We let $\widetilde{\delta} = C\delta/4$ and obtain that

$$\sum_{j=2}^{J} u_j^2 \leq C\delta \sum_{j=2}^{J} \left[\delta \left(u_{j-1}^2 + u_{j+1}^2\right) + 2\left(1 + \frac{1}{4C\delta}\right) u_j^2\right]$$

or, equivalently,

$$\sum_{j=2}^{J} u_j^2 \leq \frac{4C\delta^2}{1 - 4C\delta - 4c\delta^2} (u_1^2 + u_{J+1}^2) \leq \frac{4C\delta^2}{1 - 4C\delta - 4c\delta^2}.$$

The last inequality is because $\|\mathbf{u}\| = 1$. It remains to show that $|u_1| \sim \delta$. This follows from

$$|\Upsilon_{11}|(u_1 - u_2) = |\Lambda|u_1,$$

the estimate (4.30) that gives $|\Upsilon_{11}| = O(N)$, and the assumption $|\Lambda| = \delta/N$.

REFERENCES

[1] Shima H Abadi, Daniel Rouseff, and David R Dowling. Blind deconvolution for robust signal estimation and approximate source localizationa). *The Journal of the Acoustical Society of America*, 131(4):2599–2610, 2012.

[2] DS Ahluwalia, JB Keller, and BJ Matkowsky. Asymptotic theory of propagation in curved and nonuniform waveguides. *The Journal of the Acoustical Society of America*, 55(1):7–12, 1974.

[3] R. Alonso and L. Borcea. Electromagnetic wave propagation in random waveguides. submitted. Preprint arXiv:1310.4890v1 [math-ph].

[4] R. Alonso, L. Borcea, and J. Garnier. Wave propagation in waveguides with random boundaries. *Commun. Math. Sci.*, 11:233–267, 2012.

[5] Arthur B Baggeroer, William A Kuperman, and Peter N Mikhalevsky. An overview of matched field methods in ocean acoustics. *Oceanic Engineering, IEEE Journal of*, 18(4):401–424, 1993.

[6] L. Borcea. Imaging and wave propagation in random waveguides. Lecture notes to be published by the Societe Mathematique de France. Available to download at: http://www-personal.umich.edu/∼borcea/Publications/FRANCE_COURSE.pdf.

[7] L. Borcea and J. Garnier. Paraxial coupling of propagating modes in three-dimensional waveguides with random boundaries. *SIAM Multiscale Model. Simul.*, 12(2):832–878, 2014.

[8] L. Borcea, J. Garnier, and C. Tsogka. A quantitative study of source imaging in random waveguides. *Commun. Math. Sci.*, 2014, in press. Preprint arXiv: 1306.1544v1.

[9] L. Borcea, L. Issa, and C. Tsogka. Source localization in random acoustic waveguides. *SIAM Multiscale Model. Simul.*, 8:1981–2022, 2010.

[10] L.B. Dozier and F.D. Tappert. Statistics of normal mode amplitudes in a random ocean. *J. Acoust. Soc. Am.*, 63:533–547, 1978.

[11] S Félix and V Pagneux. Multimodal analysis of acoustic propagation in three-dimensional bends. *Wave Motion*, 36(2):157–168, 2002.

[12] J. Garnier and G. Papanicolaou. Pulse propagation and time reversal in random waveguides. *SIAM J. Appl. Math.*, 67(6):1718–1739, 2007.

[13] Josselin Garnier and Knut SØlna. Effective transport equations and enhanced backscattering in random waveguides. *SIAM Journal on Applied Mathematics*, 68(6):1574–1599, 2008.

[14] C. Gomes and K. Solna. Wave propagation in random waveguides with long-range correlations. work in progress.

[15] C. Gomez. Wave propagation in underwater acoustic waveguides with rough boundaries. Preprint arXiv: 0911.5646 [math AP].

[16] C. Gomez. Wave propagation in shallow-water acoustic random waveguides. *Commun. Math. Sci.*, 9:81–125, 2011.

[17] K.D. Heaney and WA Kuperman. Very long-range source localization with a small vertical array. *The Journal of the Acoustical Society of America*, 104:2149, 1998.

[18] J. B. Keller and J. S. Papadakis, editors. *Wave propagation in a randomly inhomogeneous ocean*, volume 70. Springer Verlag, Berlin, 1977.

[19] J.L. Krolik. Matched-field minimum variance beamforming in a random ocean channel. *The Journal of the Acoustical Society of America*, 92:1408, 1992.

[20] D. Marcuse. *Theory of dielectric optical waveguides*. Quantum electronics–principles and applications. Academic Press, 1991.

[21] Beresford N Parlett. *The symmetric eigenvalue problem*, volume 7. SIAM, 1980.

[22] Lu Ting and Michael J Miksis. Wave propagation through a slender curved tube. *The Journal of the Acoustical Society of America*, 74(2):631–639, 1983.

[23] K. Yoo and TC Yang. Broadband source localization in shallow water in the presence of internal waves. *The Journal of the Acoustical Society of America*, 106:3255, 1999.